The interpretation of pumping tests in real aquifers

Christopher J. Neville
S.S. Papadopulos & Associates, Inc.
Last update: May 16, 2014

Overview

A key assumption underlying almost all models used to interpret pumping tests is that the aquifer is homogeneous. However, a visit at any outcrop of soil or rock should be enough to convince any hydrogeologist that the subsurface is heterogeneous. The interpretation of pumping tests is frequently straightforward if water level changes are monitored in only one observation well. In this case, only one estimate of the transmissivity is obtained. The interpretation of pumping test is more challenging when multiple wells are monitored. The responses at individual observation wells will generally be variable, reflecting the underlying heterogeneity of the aquifer. Inferences of aquifer properties that are drawn from separate analyses of the responses at individual monitoring wells frequently yield inconsistent estimates of aquifer properties. When different estimates of aquifer properties are obtained the only definitive finding is that the conceptual model underlying the analysis is violated. In these cases *none* of the individual estimates of transmissivity might be reliable.

In these notes an approach is suggested that may make it possible to look beyond the variations in the responses of individual wells to estimate the representative average transmissivity of real, that is, heterogeneous, aquifers. The notes are divided into four main sections:

- The Theis (1935) model revisited;
- Pumping tests in statistically homogeneous media;
- Pumping tests in aquifers with distinct zones of different transmissivity; and
- Case study.

1. Introduction

A pumping test is not conducted to characterize the details of the subsurface; rather, it is conducted to estimate the "representative" transmissivity of a particular hydrostratigraphic unit. Here "representative" refers to an average value that provides a reliable basis for quantitative determinations at the site. This average transmissivity is also referred to as the *effective transmissivity* specified for quantitative determinations. Typical quantitative determinations include predictions of the amount of drawdown that will result when a production well is pumped on a sustained basis, the effects of pumping on adjacent wells or surface water bodies, and the rate at which groundwater might flow into an excavation.

The interpretation of pumping tests is often straightforward if water level changes are monitored in only one observation well. It is generally possible to match some portion of the drawdown data with a theoretical model such as the Theis (1935) solution. In contrast, the interpretation of pumping tests with multiple observation wells is generally not straightforward. The interpretation of pumping tests in *real* aquifers is complicated by the fact that the responses at individual observation wells are variable.

A typical analysis of the responses observed at two monitoring wells during a pumping test conducted in southern Ontario is shown in Figure 1. It is possible to achieve relatively close matches between the observations and the Theis solution. However, as shown in the figure, the parameters estimated for both wells are different. The transmissivity estimated for OW121-50 is about double the estimate for OW119-27 and the storage coefficient is almost a factor of 100 larger. The Theis solution is founded on the assumption that the aquifer is homogeneous. A fundamental assumption of the Theis solution, and most other analytical models of pumping, is that the aquifer is homogeneous. The only conclusion that can be drawn from the analysis presented in Figure 1 is that the assumption of homogeneity is violated. Despite the good individual fits, the transmissivity estimates may be suspect as application of the Theis solution in this case does not appear to be warranted.

In the next section the Theis analysis is revisited, with the focus directed to a "historical" bur rarely used approach for interpreting the data from multiple observation wells.

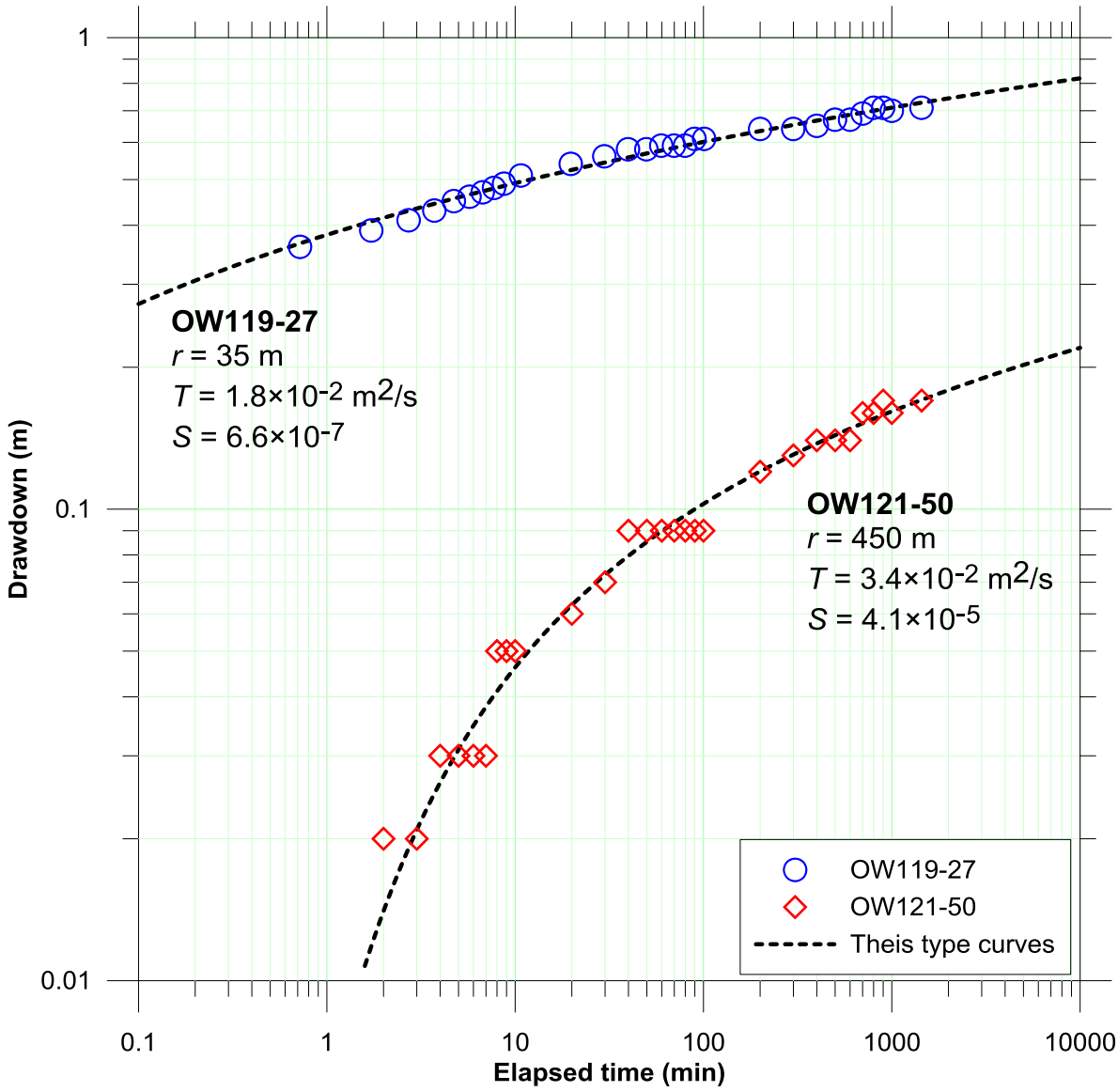

Figure 1. Example application of the Theis analysis with two observation wells

2. The Theis (1935) model revisited

The Theis (1935) model is the foundation on which all other analytical models of aquifer response to pumping are built. The Theis model is an appropriate starting point because it provides a benchmark against which the observed responses to pumping can be assessed and conditions at a site can be diagnosed. The Theis continues to be used widely in practice. Although its underlying assumptions are quite restrictive, there is generally a portion of the test response for which the assumptions are not violated too severely.

The conceptual model of the aquifer in the Theis model is illustrated schematically in Figure 2.

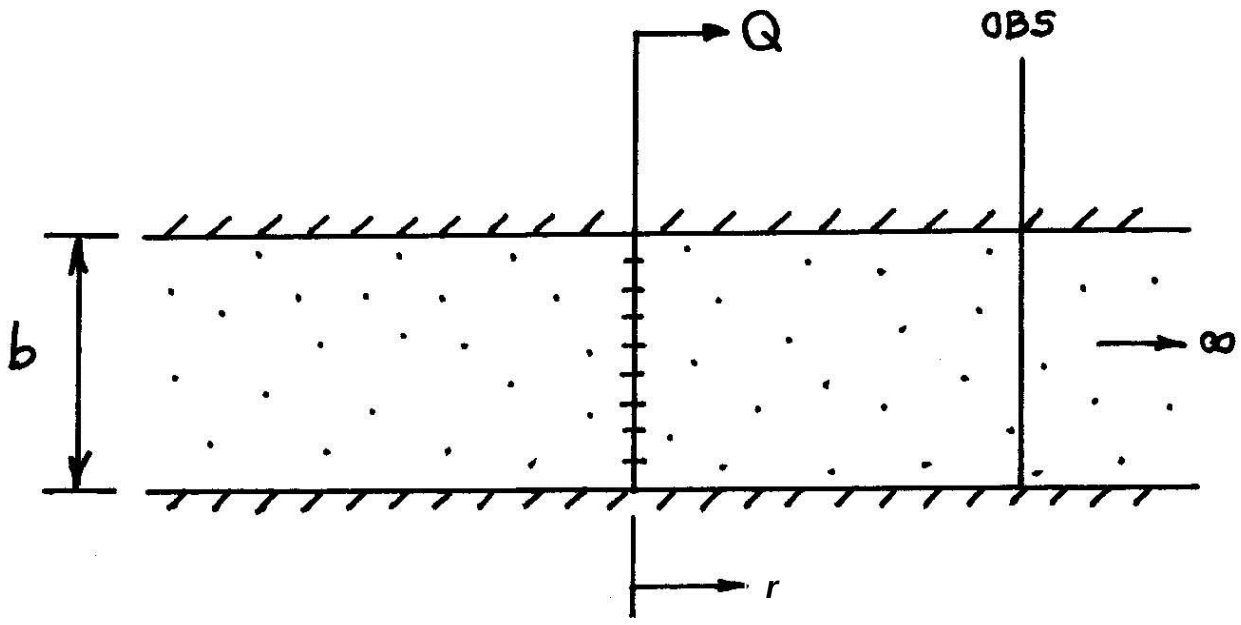

Figure 2. Conceptual model for the Theis (1935) model

The Theis model incorporates the following assumptions about the aquifer:

- The transmissivity is uniform;
- The transmissivity is isotropic;
- The aquifer is infinite in areal extent;
- The aquifer is perfectly confined by impermeable strata above and below;
- The head in the pumped aquifer always remains above the top of the aquifer; and
- The release of water from storage is governing by linear constitutive relations with properties that remain constant through time.

For a pumping well idealized as a line-sink that penetrates the full thickness of the aquifer, the drawdown, *s*, at any distance from the pumping well, *r*, and elapsed time *t* since the start of pumping is given by:

$$s(r,t) = \frac{Q}{4\pi T}\left[-Ei\left\{-\frac{r^2 S}{4Tt}\right\}\right] \tag{1}$$

Here *Q* is the pumping rate, *T* is the transmissivity *S* is the storage coefficient, and *Ei*(•) is the exponential integral:

$$Ei(x) = \int_{-\infty}^{x} \frac{1}{y} EXP\{-y\}\, dy \tag{2}$$

Hydrogeologists write their version of this solution as:

$$s(r,t;u) = \frac{Q}{4\pi T} W(u) \tag{3}$$

with *W(u)* referred to as the Theis well function, defined as *–Ei(-u)*. The argument of the Theis well function, *u*, is:

$$u = \frac{r^2 S}{4Tt} \tag{4}$$

It is important to note that the argument for the Theis well function is expressed in terms of the ratio t/r^2. The solution predicts that the drawdowns for all observation wells completed in the same homogenous aquifer should fall on the same curve if they are plotted on an axis of t/r^2. To illustrate this point, a simple example illustrated in Figure 3 is considered. A fully penetrating well is pumped at a constant rate, and the drawdown is monitored at four observation wells.

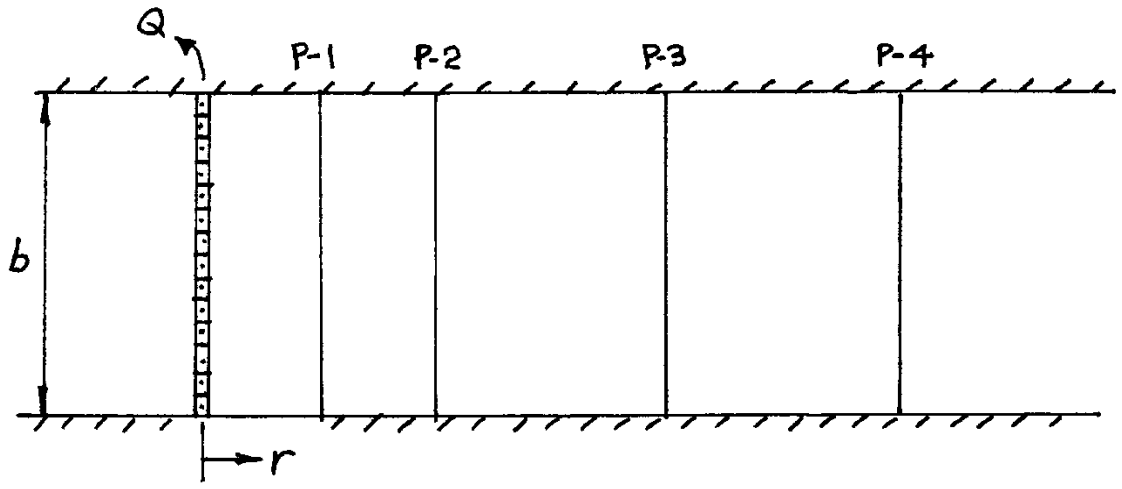

Figure 3. Conceptual model for the example calculations

For the example, the transmissivity and storativity are 10^{-4} m^2/s and 10^{-4}, respectively. The well is pumped at a constant rate of 5×10^{-4} m^3/s. The observation wells are located at the following distances:

- P-1: r = 5.0 m;
- P-2: r = 10.0 m;
- P-3: r = 20.0 m; and
- P-4: r = 30.0 m;

The time-drawdown records for the individual wells are plotted in Figure 4.

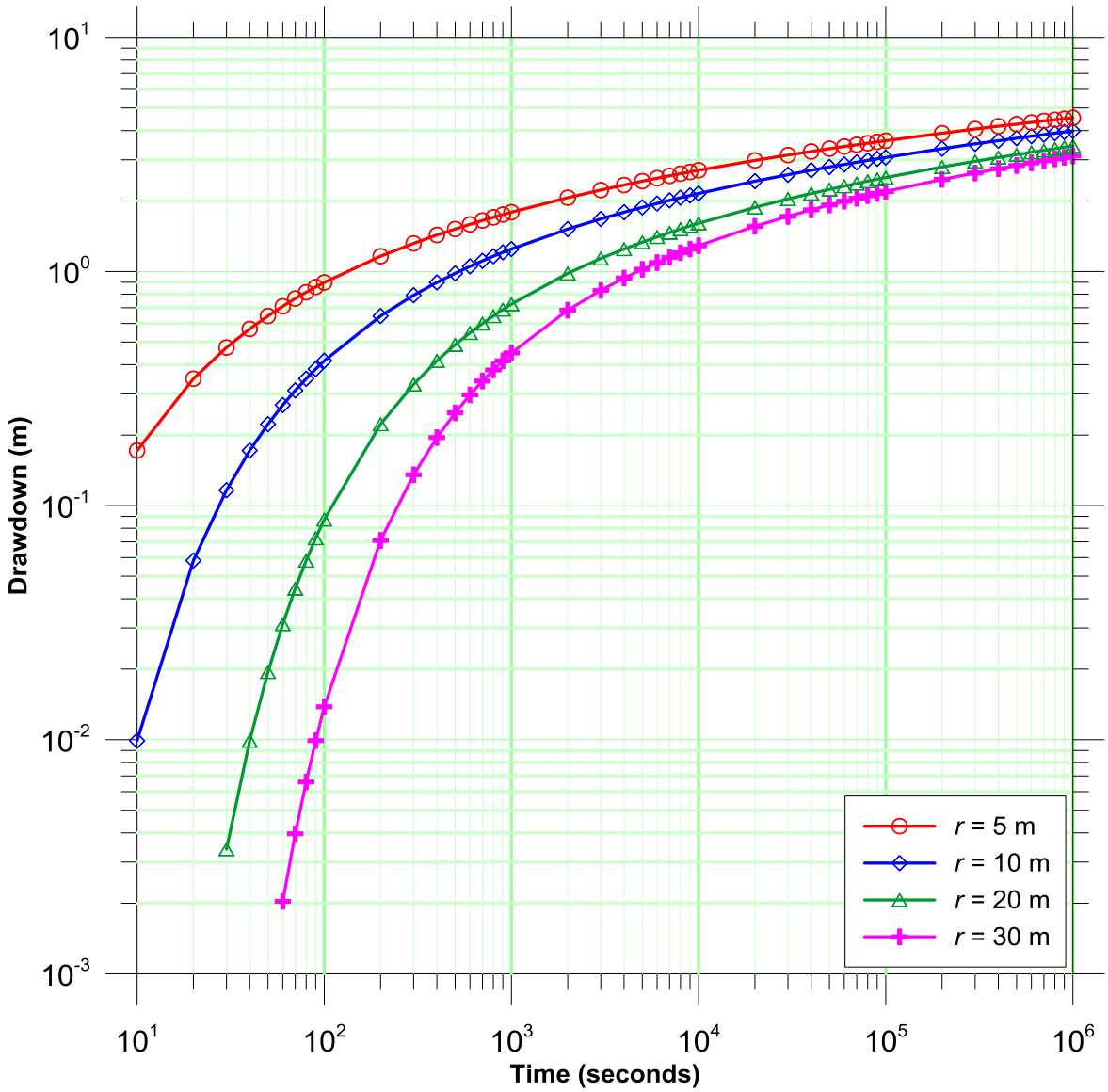

Figure 4. Calculated drawdowns at observation wells

In Figure 5, the drawdowns for the individual monitoring wells are re-plotted against t/r^2 instead of t. As predicted by the theory, the drawdowns collapse to a single curve. A plot of the drawdowns against t/r^2 is referred to as a *composite* plot (Cooper and Jacob, 1946).

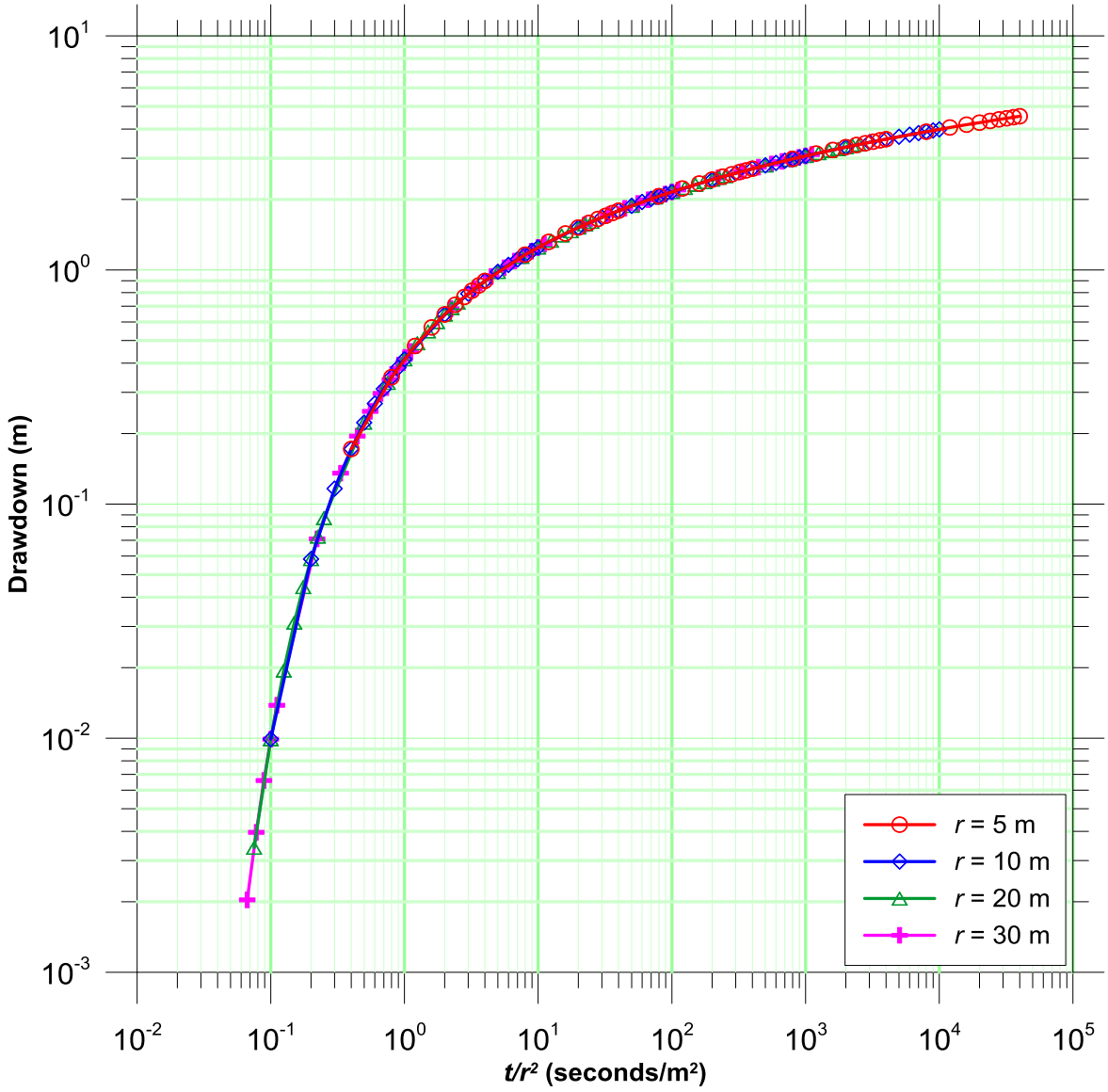

Figure 5. Drawdown data plotted vs. t/r^2

Cooper and Jacob (1946) suggested that for u less than a certain value, the Theis well function could be approximated by the first two terms of its series expansion:

$$W(u) \cong -0.5772 - \ln\{u\}$$
$$= -0.5772 + \ln\left\{\frac{1}{u}\right\}$$

The limit of applicability of the Cooper-Jacob approximation is typically cited to be $u < 0.01$ ($1/u > 100$) [see for example, Todd and Mays (2005)]. However, as shown in Figure 6, the Cooper and Jacob approximation is still very close for larger values of u. For example, for $u = 0.1$ ($1/u = 10$), the error in the approximation is still only about 5%.

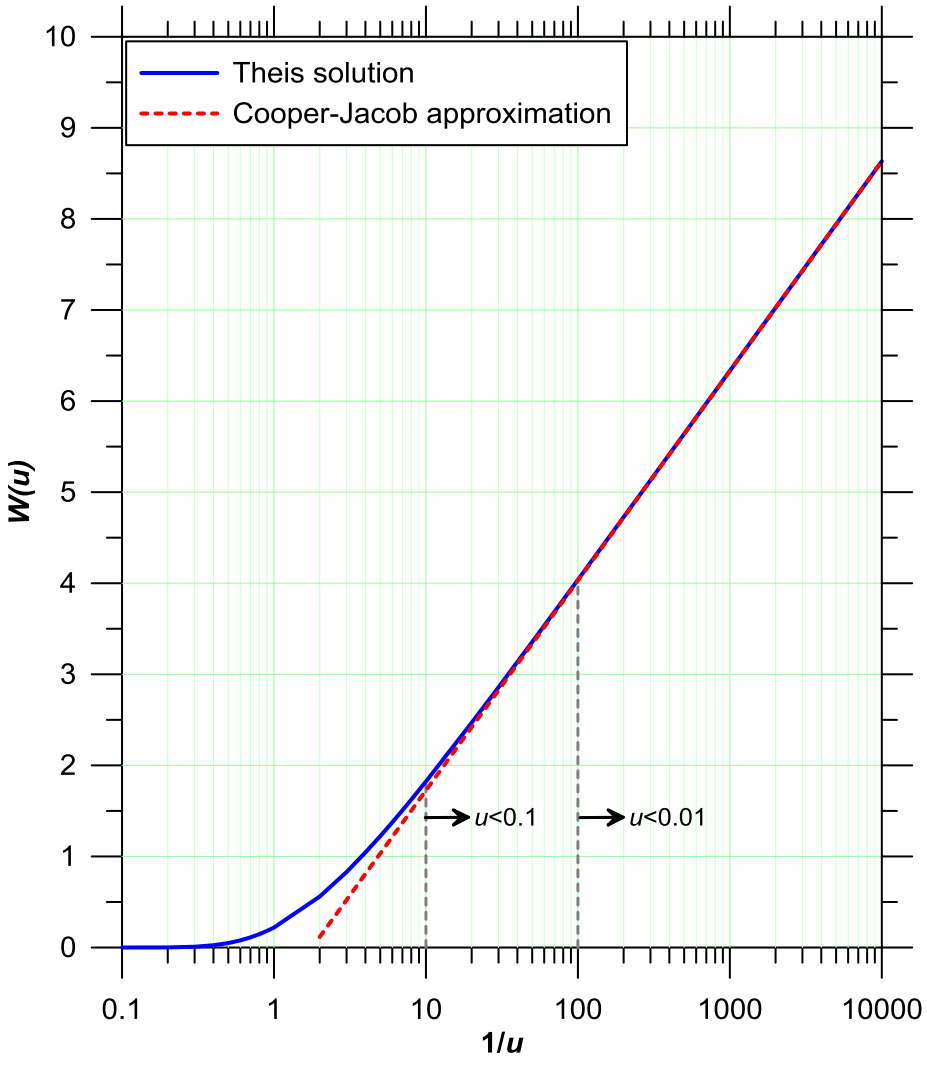

Figure 6. Cooper-Jacob approximation of the Theis well function

The Cooper-Jacob analysis can also be applied for a composite plot. The Cooper-Jacob approximation of the Theis solution can be written as:

$$s = \frac{Q}{4\pi T} 2.303 \log_{10}\left[2.2459 \frac{T}{S}\left(\frac{t}{r^2} \right) \right] \qquad (5)$$

The composite Cooper-Jacob semilog plot of the drawdowns plotted in Figure 4 is shown in Figure 7. Beyond the limit of applicability of the Cooper-Jacob approximation, the drawdowns collapse to a single straight line when plotted against the logarithm of t/r^2.

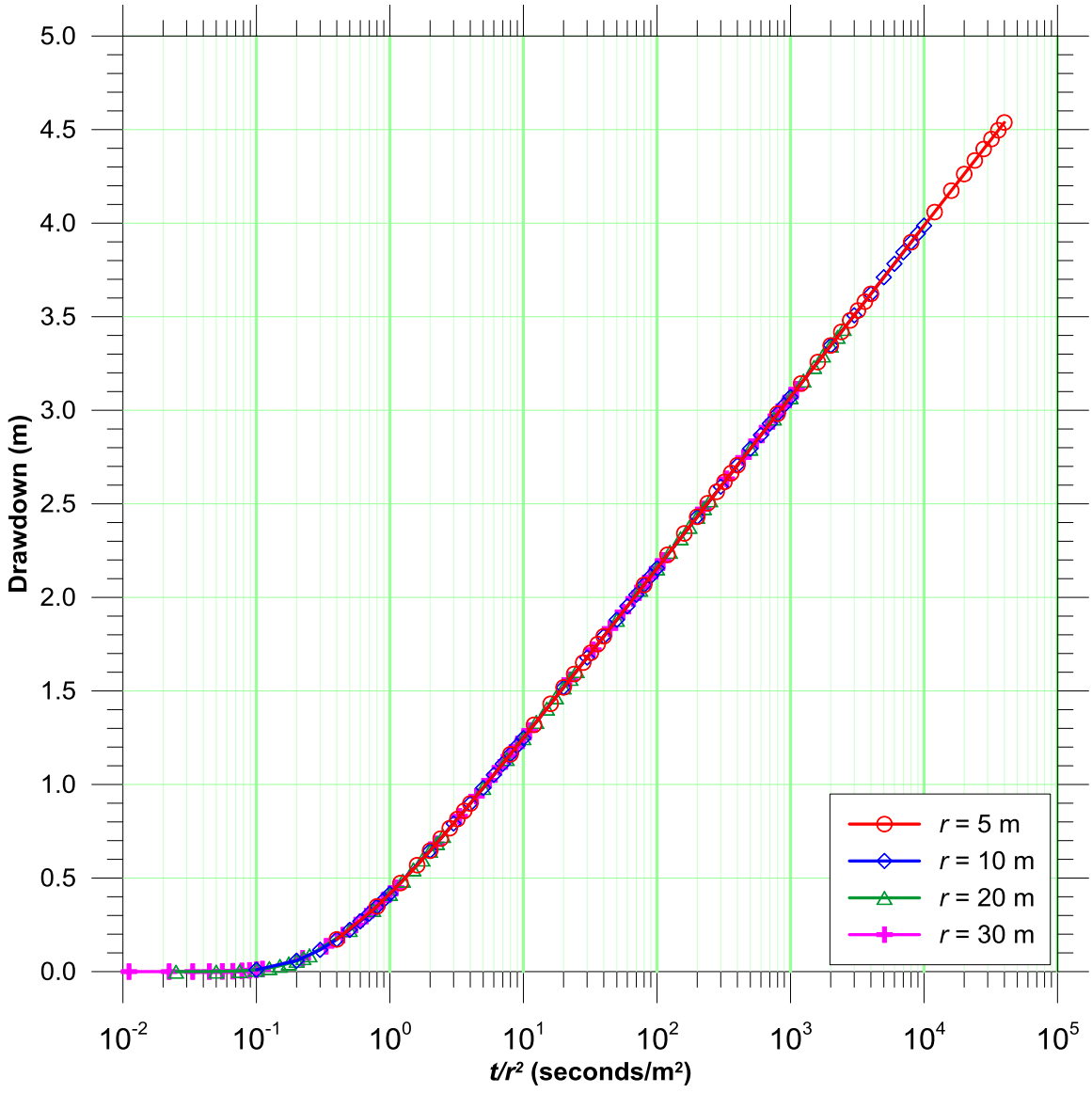

Figure 7. Drawdown data plotted vs. t/r^2

The Cooper-Jacob analysis for a composite plot is essentially identical to the time-drawdown analysis for a single well. Differentiating the Cooper-Jacob approximation with respect to $\log\left(\frac{t}{r^2}\right)$ yields:

$$\frac{\partial s}{\partial\left(\log\frac{t}{r^2}\right)} = 2.303\frac{Q}{4\pi T}$$

Solving for *T*:

$$T = 2.303\frac{Q}{4\pi}\left(\frac{\partial s}{\partial\left(\log\frac{t}{r^2}\right)}\right)^{-1} = 2.303\frac{Q}{4\pi}\left(SLOPE\big|_{t/r^2}\right)^{-1} \qquad (6)$$

The storage coefficient is estimated by extrapolating the semilog plot back to zero drawdown:

$$S = 2.2459T\left(\frac{t}{r^2}\right)_0 \qquad (7)$$

A Cooper-Jacob analysis for the results assembled on the composite semilog plot of Figure 7 is presented in Figure 8. The slope of the straight line yields the transmissivity specified in the generation of the results shown in Figure 4.

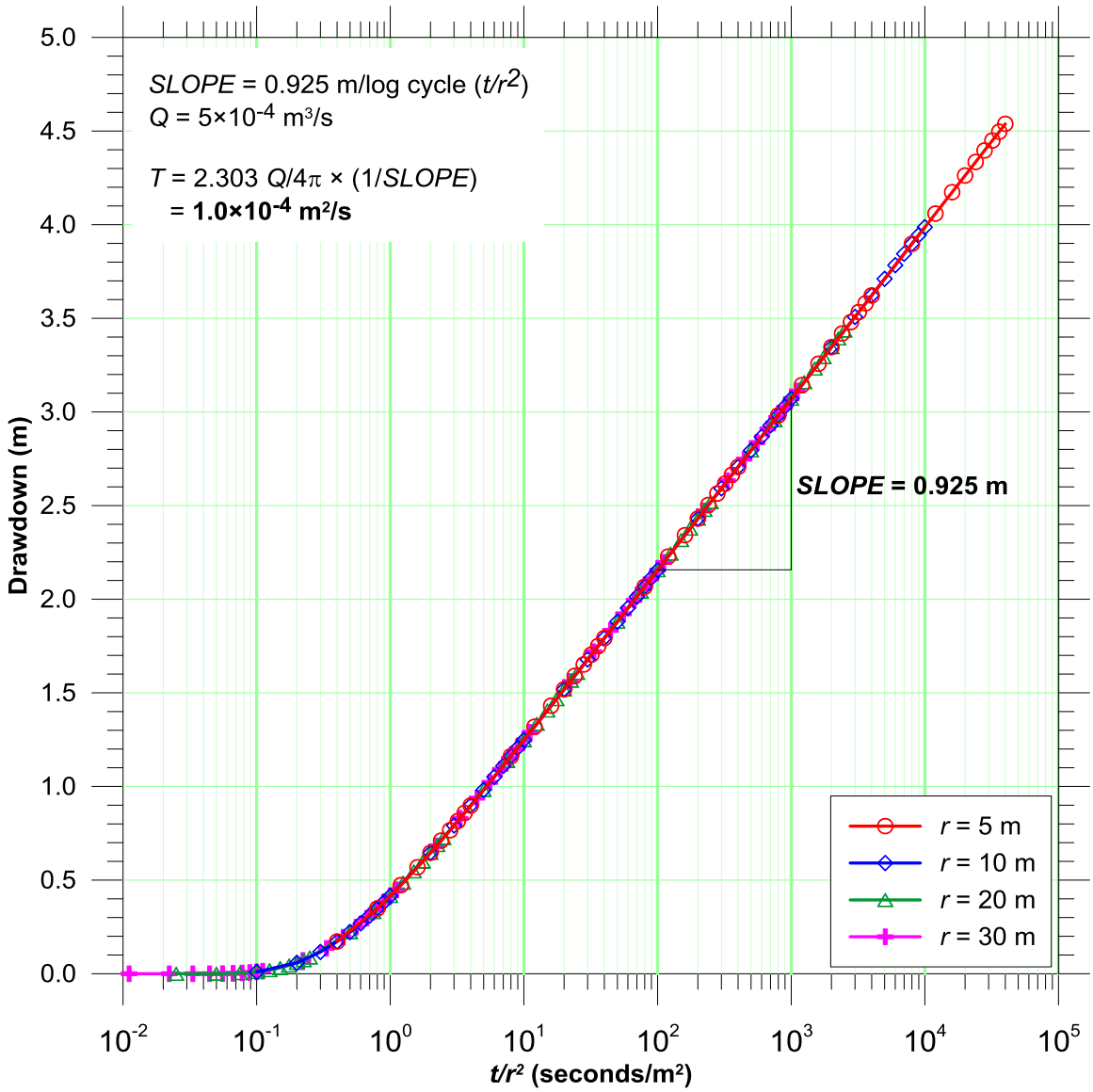

Figure 8. Cooper-Jacob composite analysis

It is important to note that composite plots are not new. In their seminal paper, Cooper and Jacob (1946) indicated that this approach for plotting drawdown data should be adopted when drawdowns are available for several observed wells at different times. Weeks (1977) had some incisive comments on composite plots:

> *The composite data-curve matching process is also important during the analysis of the test data. Such a match should always be made when data from more than one observation well are available, and single values of transmissivity, storage coefficient, and other hydraulic properties are to be determined from that data.*

Moench (2010) indicates that use of a composite plot is an essential element for analysis as it allows for input from an experienced hydrogeologist to account for non-ideal aquifer conditions.

An approach for interpreting pumping tests with multiple observation wells is shown in Figure 9 for the example considered in Figure 1. The dashed lines shown in the figure do not represent lines-of-best-fit. Rather, they are parallel lines constructed so that they approximate the observations from both observations wells. Referring to Equation (6), both lines will yield the same estimate of transmissivity; this estimate is interpreted as the bulk-average transmissivity. The dashed lines yield different estimates of the storage coefficient; this inconsistency is interpreted to be diagnostic of aquifer heterogeneity. The remaining sections of these notes are devoted to assessing whether these interpretations are appropriate.

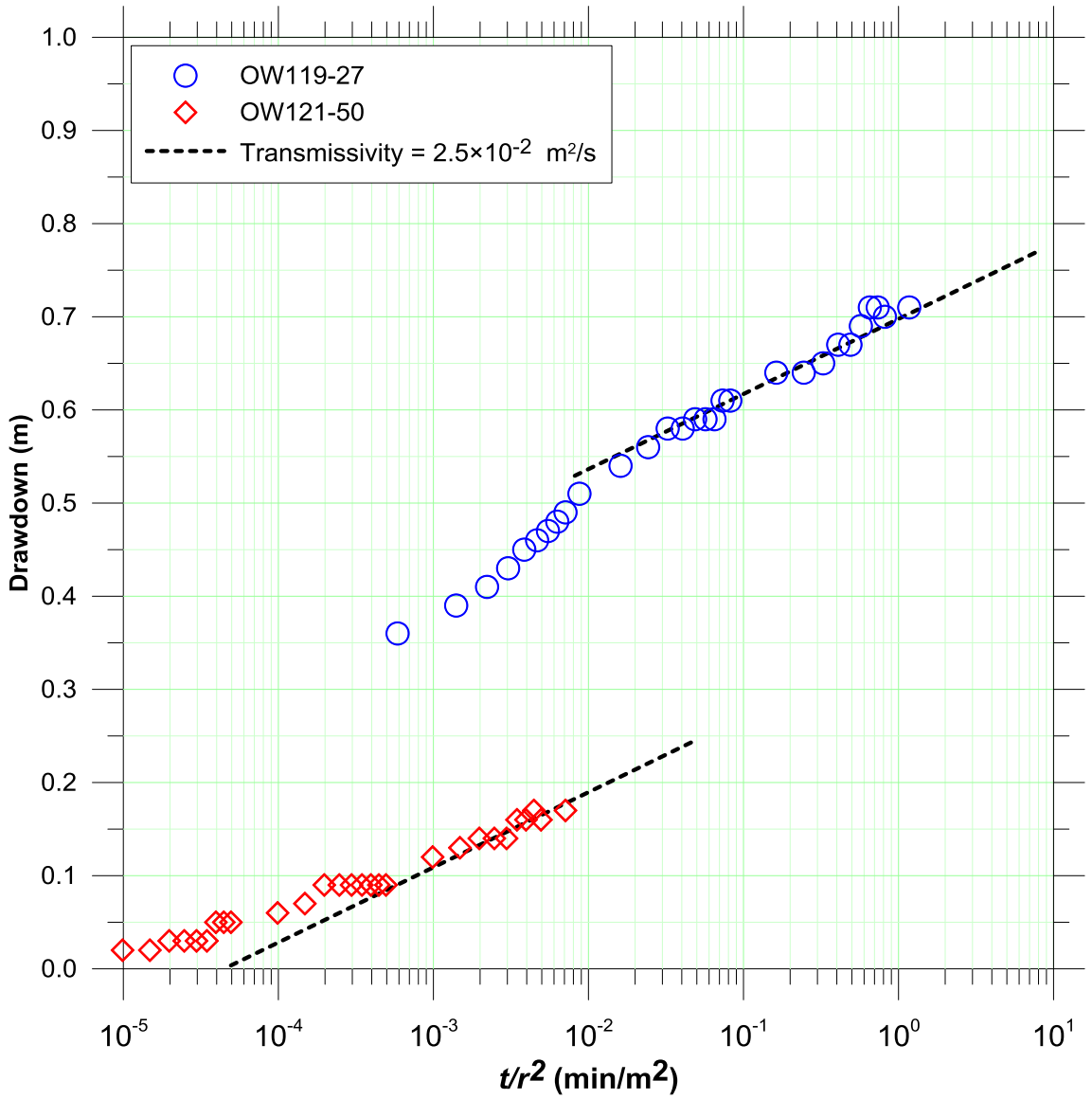

Figure 9. Cooper-Jacob composite analysis with consistent transmissivity estimates

3. Pumping tests in statistically homogeneous media

Researchers in stochastic hydrology have examined through numerical simulations the influence of aquifer heterogeneity on the responses to pumping. An important assumption in these simulations is that the aquifer is statistically homogeneous. Within a particular hydrostratigraphic unit it may be possible to conceive of the small-scale variations in transmissivity as a random field with spatial correlation but there are no large-scale trends in the hydraulic conductivity or distinct zones with different properties.

Meier and others (1998) simulated pumping tests in heterogeneous aquifers in which the transmissivity is represented as a random correlated field with an underlying lognormal distribution. They used a plan-view numerical model to simulate pumping from a central well in random fields of hydraulic conductivity. The hydraulic conductivity was assumed to be log-normally distributed with a geometric mean transmissivity, T_G, of 1.0, and variances of log-transmissivity, σ_Y^2, of 0.25 and 4.0 (Meier and others (1998) adopted general consistent units). The transmissivity distribution for a log-variance of 4.0 is reproduced in Figure 10. The detailed distribution around the pumping well is shown in the inset.

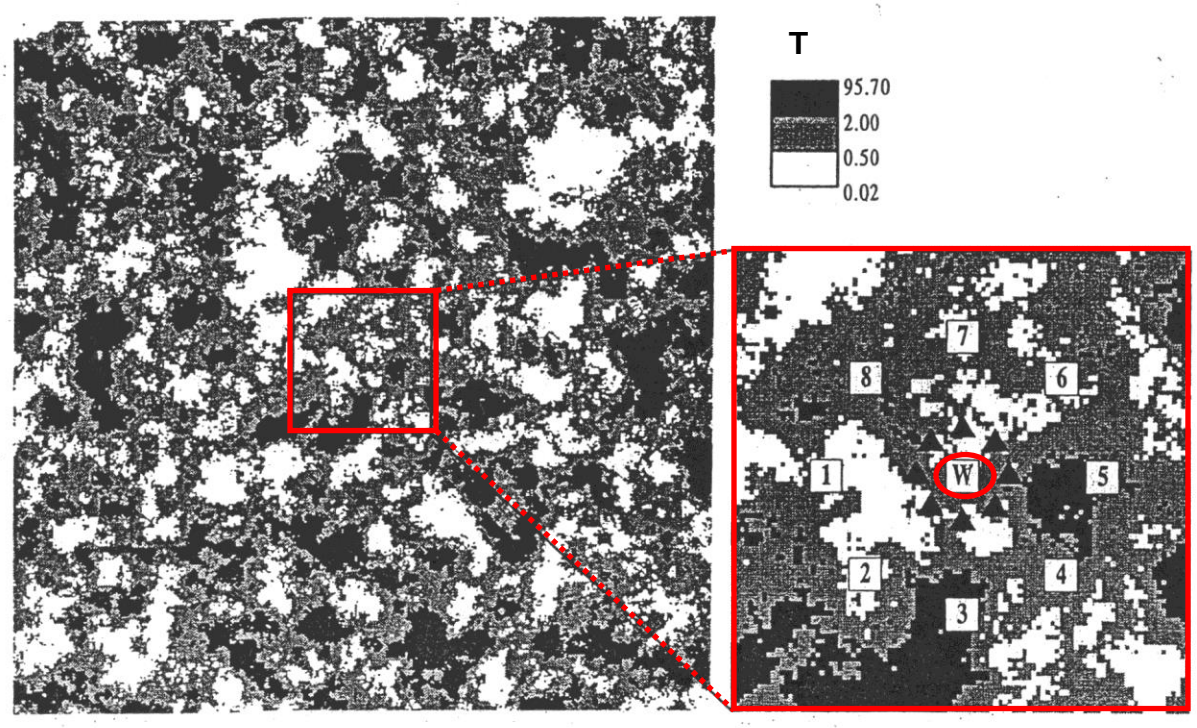

Figure 10. Random transmissivity field for σ_Y^2 = 4.0
(Adapted from Meier and others, 1998; Figure 8)

Case 1: $\sigma_Y^2 = 0.25$

The cumulative probability density function for $T_G = 1.0$ and $\sigma_Y^2 = 0.25$ is plotted in Figure 11. As shown in this figure, the spread of the transmissivity values about the mean value is relatively narrow.

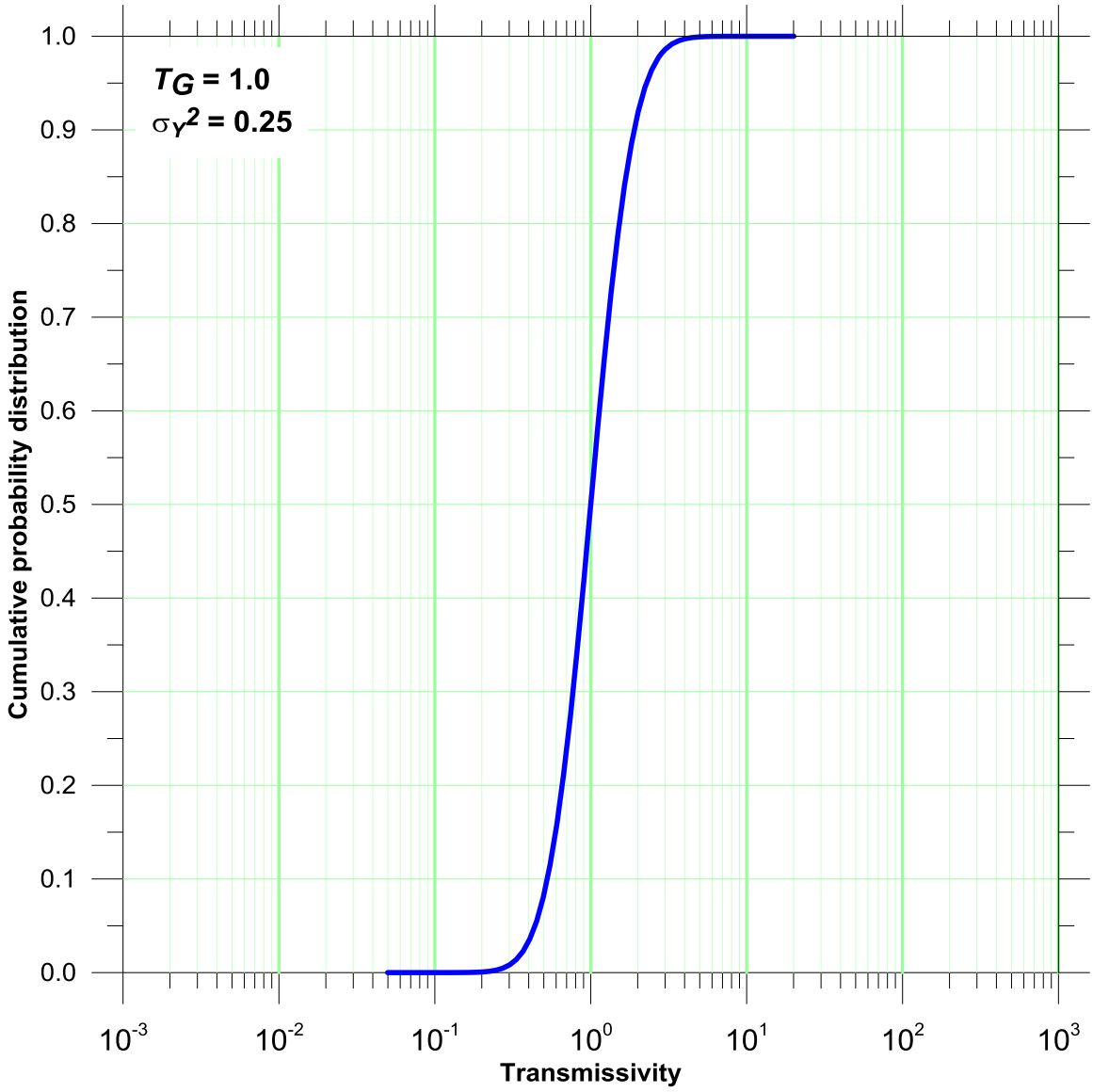

Figure 11. Cumulative probability density function of transmissivity for $\sigma_Y^2 = 0.25$

The plot of the drawdowns simulated by Meier and others (1998) for $\sigma_Y^2 = 0.25$ is reproduced in Figure 12. The solid line shown in the figure denotes the response predicted for an aquifer that has a uniform transmissivity given by the geometric mean of the random field, T_G. The individual time-drawdown records at distances of 10 and 30 are approximately parallel to each other and to the lines calculated for a uniform transmissivity. This implies that consistent estimates of transmissivity will be obtained from Cooper-Jacob semilog straight-line analyses.

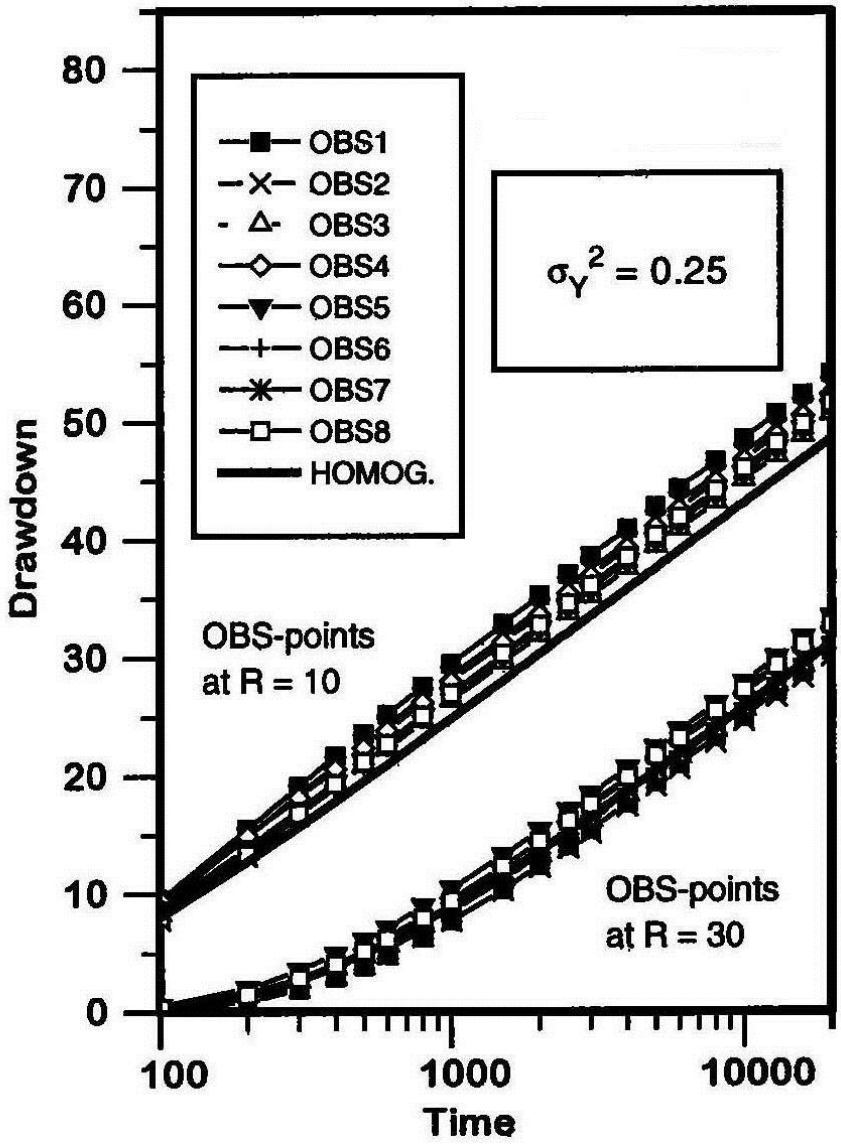

Figure 12. Simulated drawdowns for σ_Y^2=0.25
(Reproduced from Meier and others, 1998; Figure 8)

The simulated drawdowns for σ_Y^2 = 0.25 have been digitized and are assembled in a composite plot in Figure 13. The drawdowns from all of the wells approximate a single straight line. As shown in Figure 14, for this case of a relatively small variance of log-transmissivity, the simulated responses for the individual monitoring locations can be matched closely with the Theis solution evaluated with the geometric mean transmissivity, T_G = 1.0.

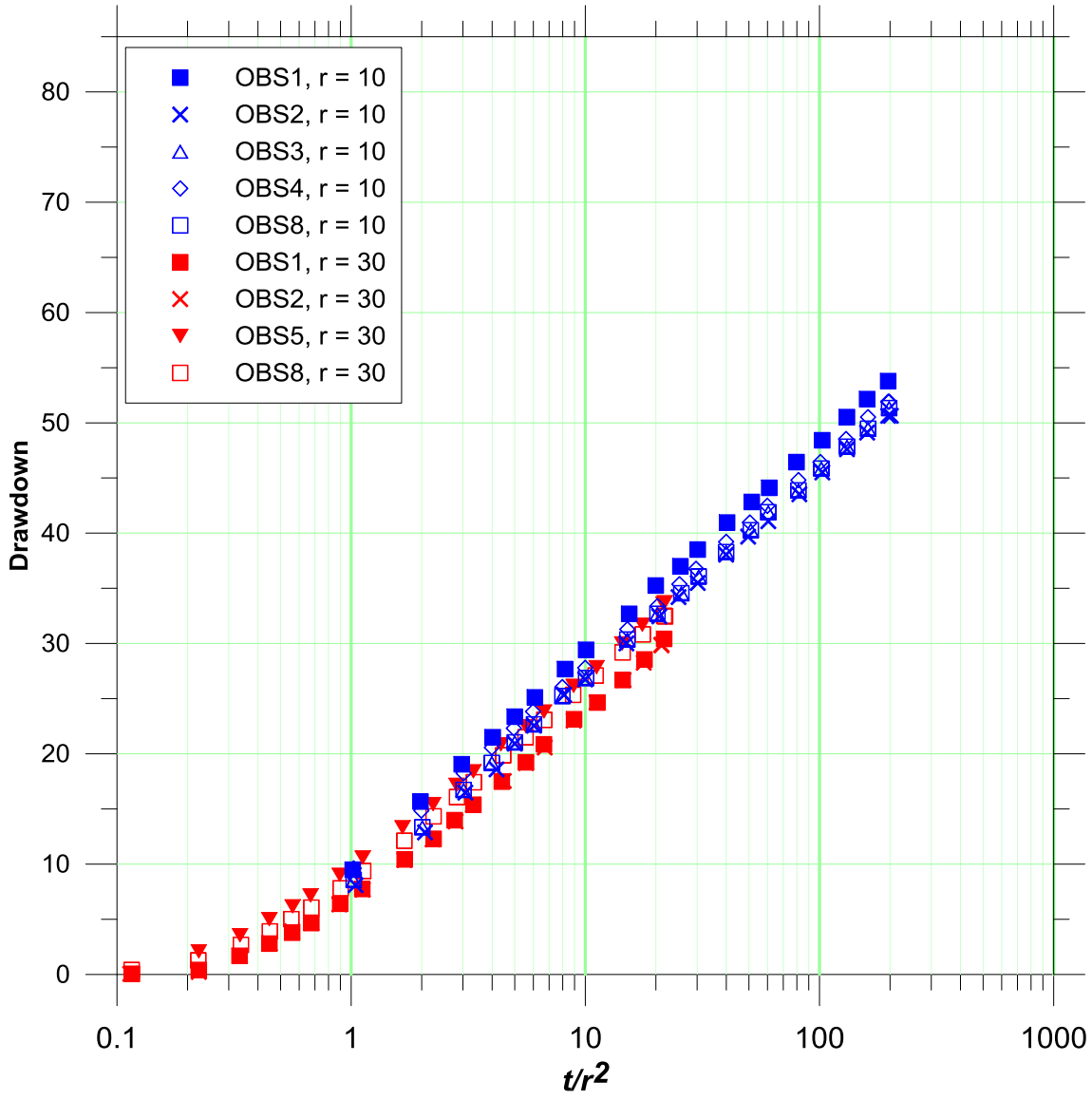

Figure 13. Composite plot of drawdowns for σ_Y^2=0.25

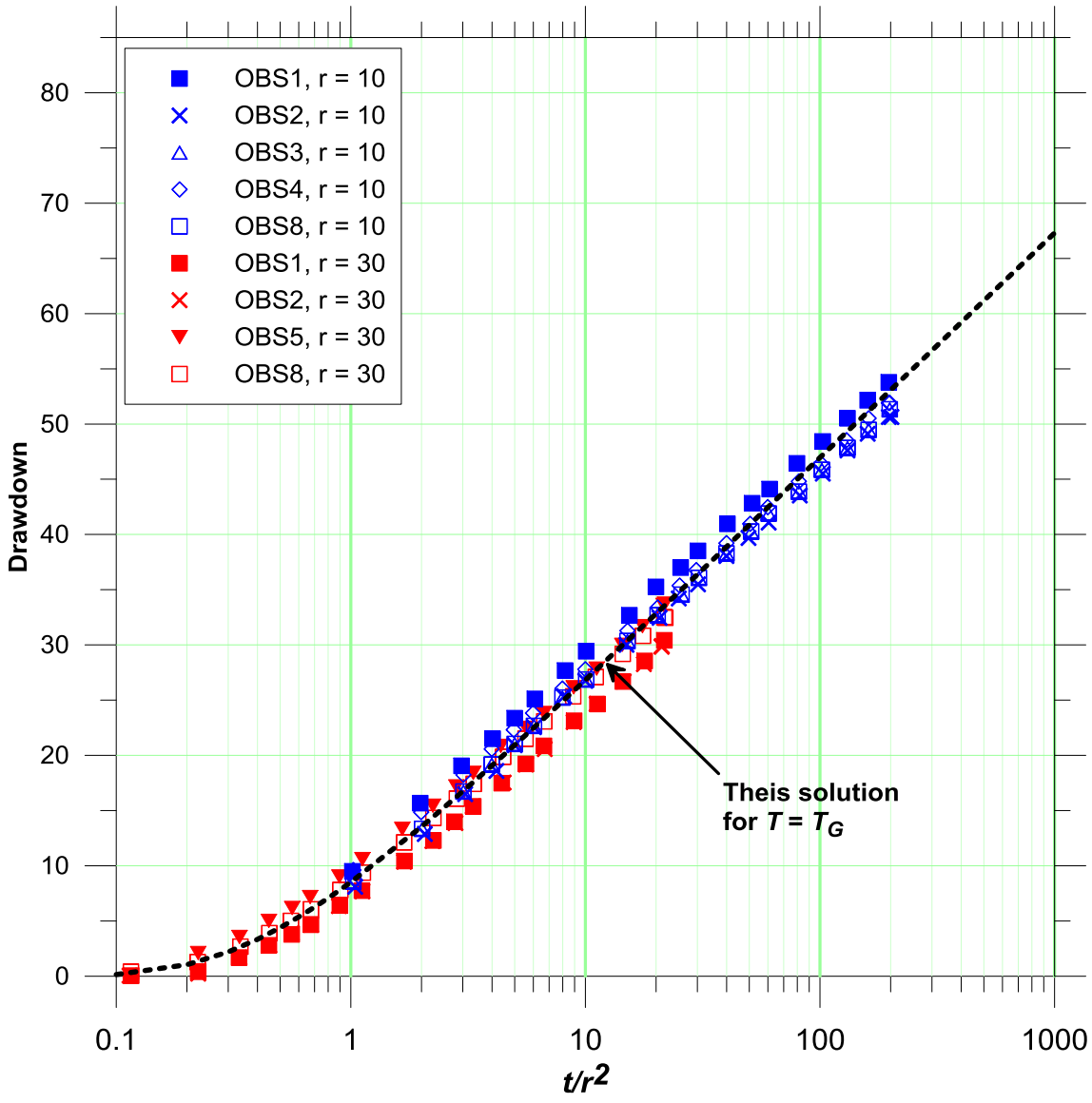

Figure 14. Composite plot of drawdowns for σ_Y^2=0.25 with Theis solution for T_G

Case 2: $\sigma_Y^2 = 4.0$

The cumulative probability density function for $\sigma_Y^2 = 4.0$ is plotted in Figure 15. The cumulative probability distribution for σ_Y^2=0.25 is also shown for comparison. The distribution for a variance of 4.0 is relatively broad, indicating that the point values of transmissivity may vary over several orders of magnitude.

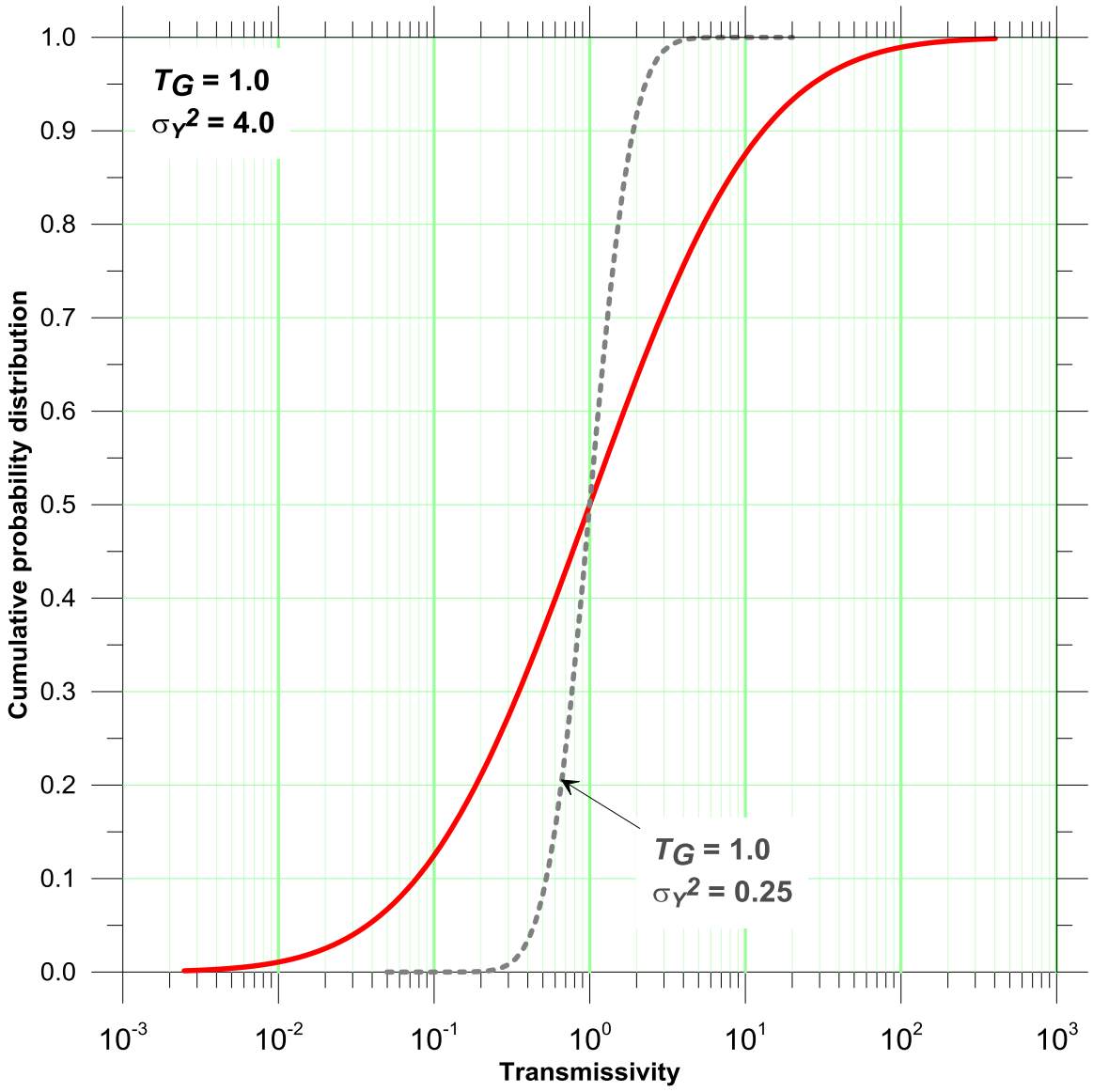

Figure 15. Cumulative probability density function of transmissivity for $\sigma_Y^2 = 4.0$

Meier and others (1998) plot of the simulated drawdowns for $\sigma_Y^2 = 4.0$ are reproduced in Figure 16. There is a significant spread in the drawdowns at the different observation wells located the same distance from the pumping well. The different storativities reflect the fact that the time required for a pressure pulse to migrate to different points in the aquifer will differ, characteristic of a heterogeneous aquifer.

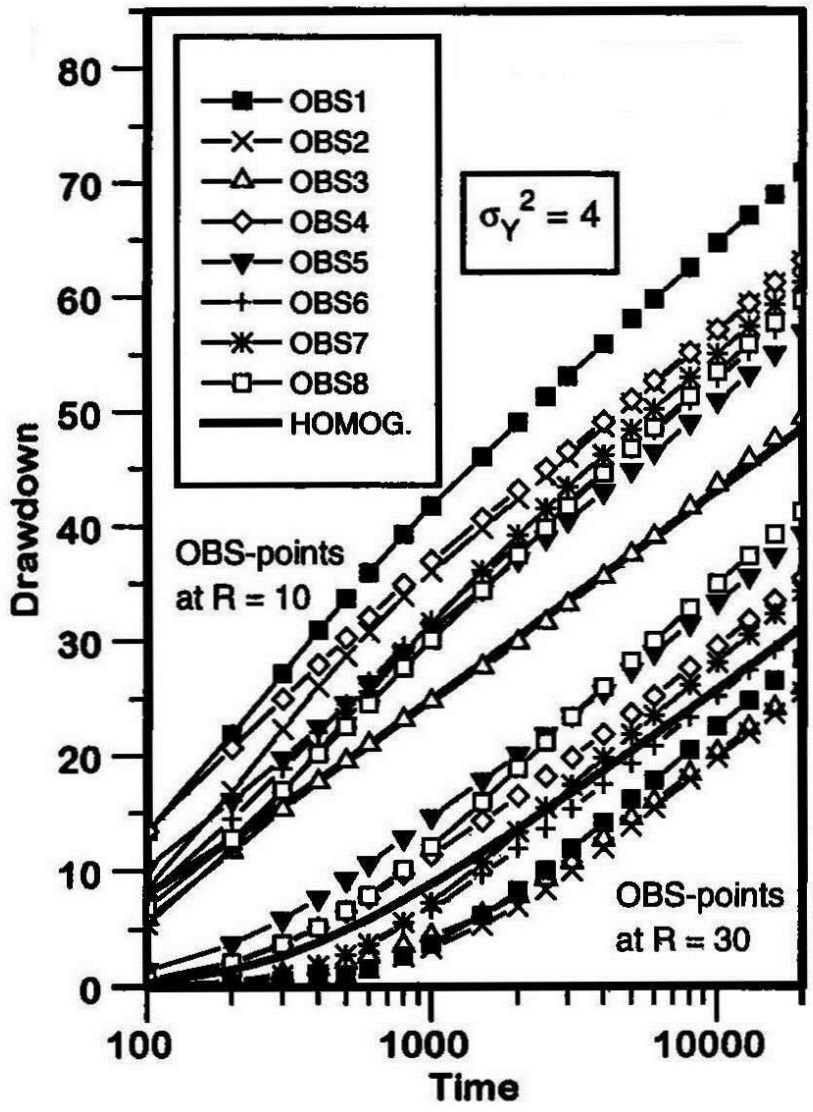

Figure 16. Simulated drawdowns for σ_Y^2=4.0
(Reproduced from Meier and others, 1998; Figure 8)

The simulated drawdowns for σ_Y^2= 4.0 are assembled on a composite plot in Figure 17. For the case of a relatively high variance of σ_Y^2= 4.0, the individual time-drawdown records do not converge on a single line on the semilog plot; however, the responses of the wells have similar later-time slopes. Cooper-Jacob analyses based on the later-time portions of the records of the individual time-drawdown records will yield similar transmissivities but different storativities.

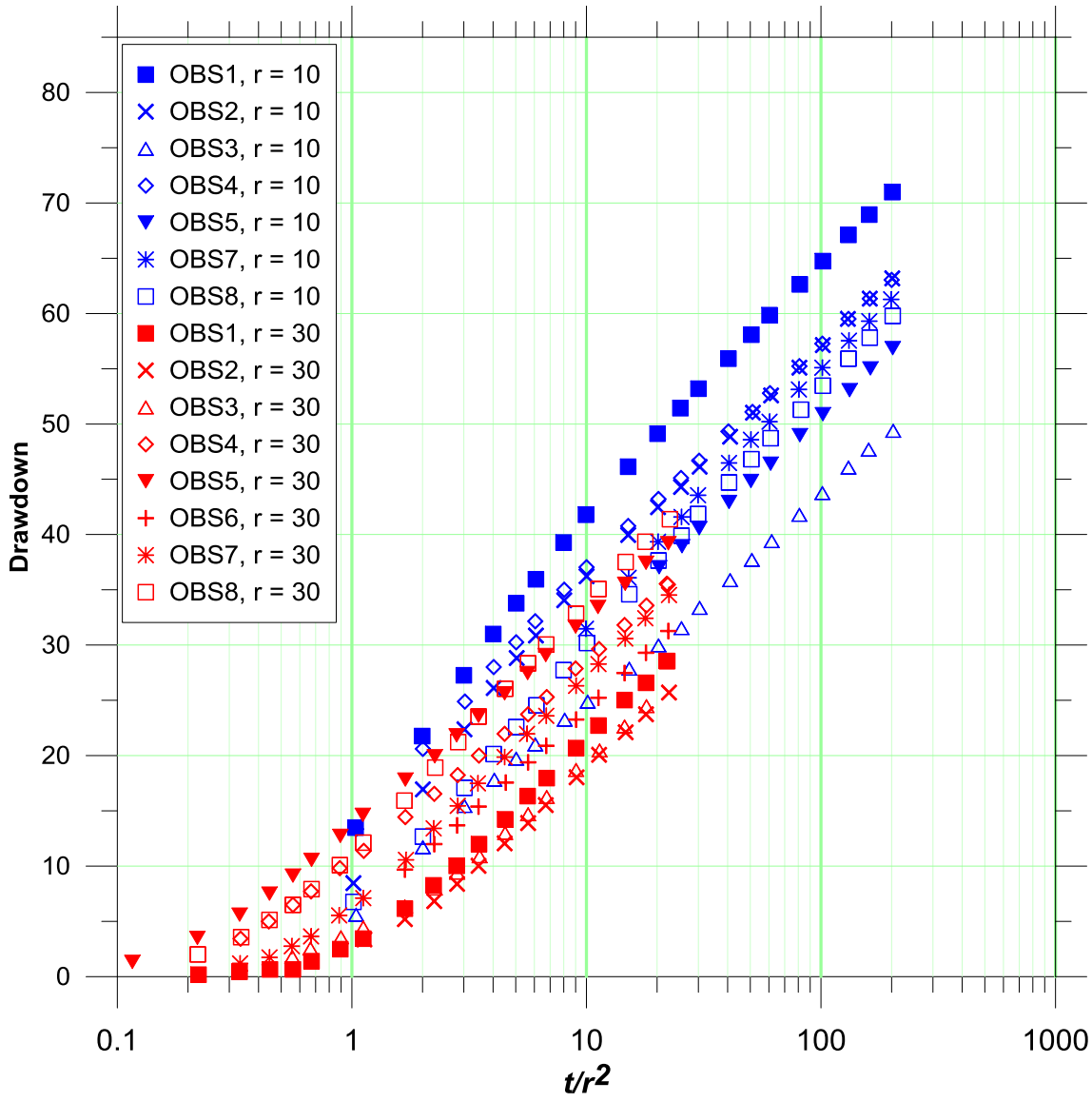

Figure 17. Composite plot of drawdowns for σ_Y^2=4.0

As shown in Figure 18, for this case of a relatively large variance of log-transmissivity, the results for the individual observation locations exhibit considerable scatter in their absolute magnitudes. However, the slopes are consistent with a bulk-average transmissivity corresponding to the geometric mean transmissivity.

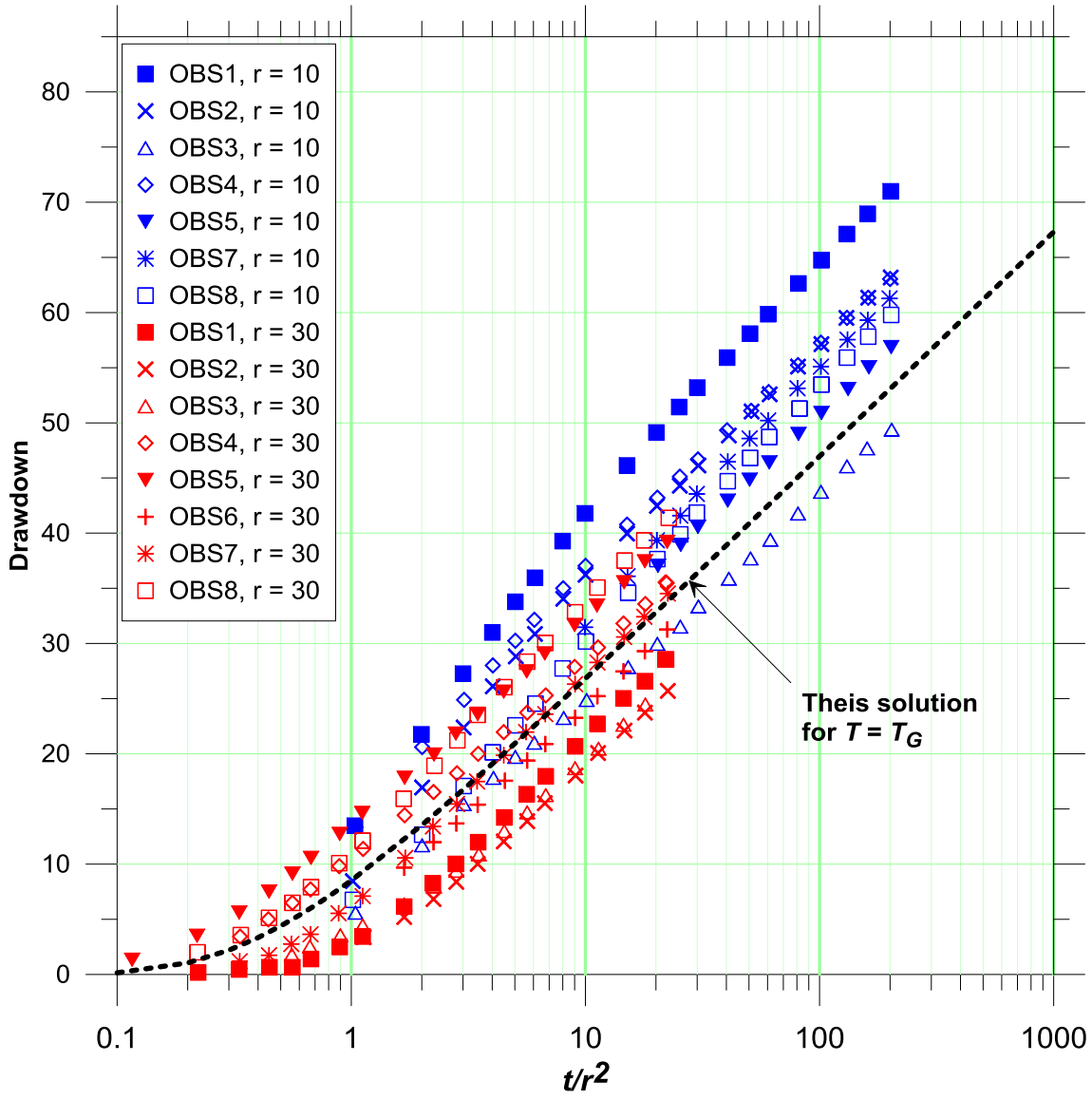

Figure 18. Composite plot of drawdowns for σ_Y^2=4.0 with Theis solution for T_G

Tentative conclusion:

The results of the simulations of Meier and others (1998) suggest that it is possible to estimate an effective transmissivity from a pumping test in a synthetic homogeneously heterogeneous aquifer, even for aquifers in which the degree of heterogeneity is relatively large.

Sánchez-Vila and others (1999) followed the numerical experiments of Meier and others (1998) with a theoretical analysis that examined in more detail what can be obtained from the Cooper-Jacob analysis. Their theoretical analyses confirmed the results of their simulations: estimated transmissivities for different observation wells tend to converge to a single value, which for a log-transformed field of transmissivity values corresponds to the geometric mean of the underlying random process.

4. Pumping tests in aquifers with zones of different transmissivity

Dr. James J. Butler and his colleagues at the Kansas Geological Survey have developed analytical solutions for an important class of problems involving transient flow to a well in heterogeneous aquifers with distinct zones of differing material properties (Butler, 1988; Butler and Liu, 1991; Butler and Liu, 1993). The solution of Butler and Liu (1993) is used here to simulate two cases involving a circular zone that has properties different from the rest of the formation. The circular zone of different properties is referred to here as a *pod*. In the first case, the pumping well is located within a pod. In the second case, an observation well is located within a pod.

Case 1: Pumping well located in a pod

The conceptual model for Case #1 is shown in Figure 19. The transmissivity of the formation is T_2 = 100 m^2/day. The pumping well is located at the center of a circular pod of 5 m radius that has a significantly lower transmissivity, T_1 = 0.1 m^2/day. A uniform storage coefficient $S_1 = S_2 = 5\times10^{-4}$ is assumed. All four of the observation wells are located outside of the pod. The well is pumped at a constant rate of 100 m^3/day.

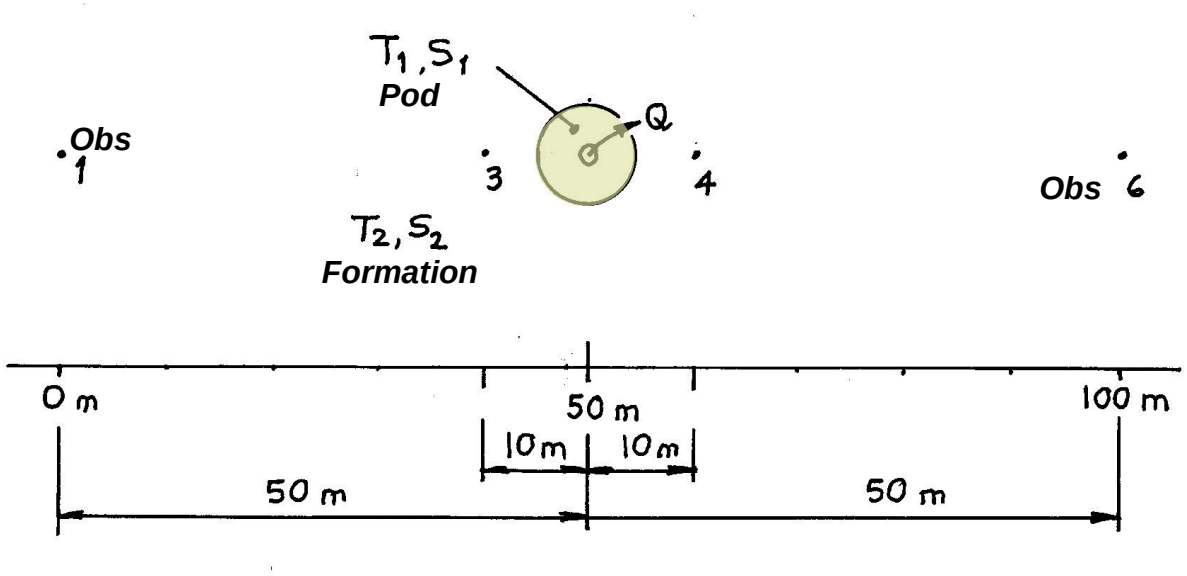

Figure 19. Conceptual model for Case #1 pod simulation

The simulated drawdowns are plotted in Figure 20. Since the observation wells are symmetric with respect to the pumping well and the pod, only the drawdowns for observation wells #1 and #3 are plotted.

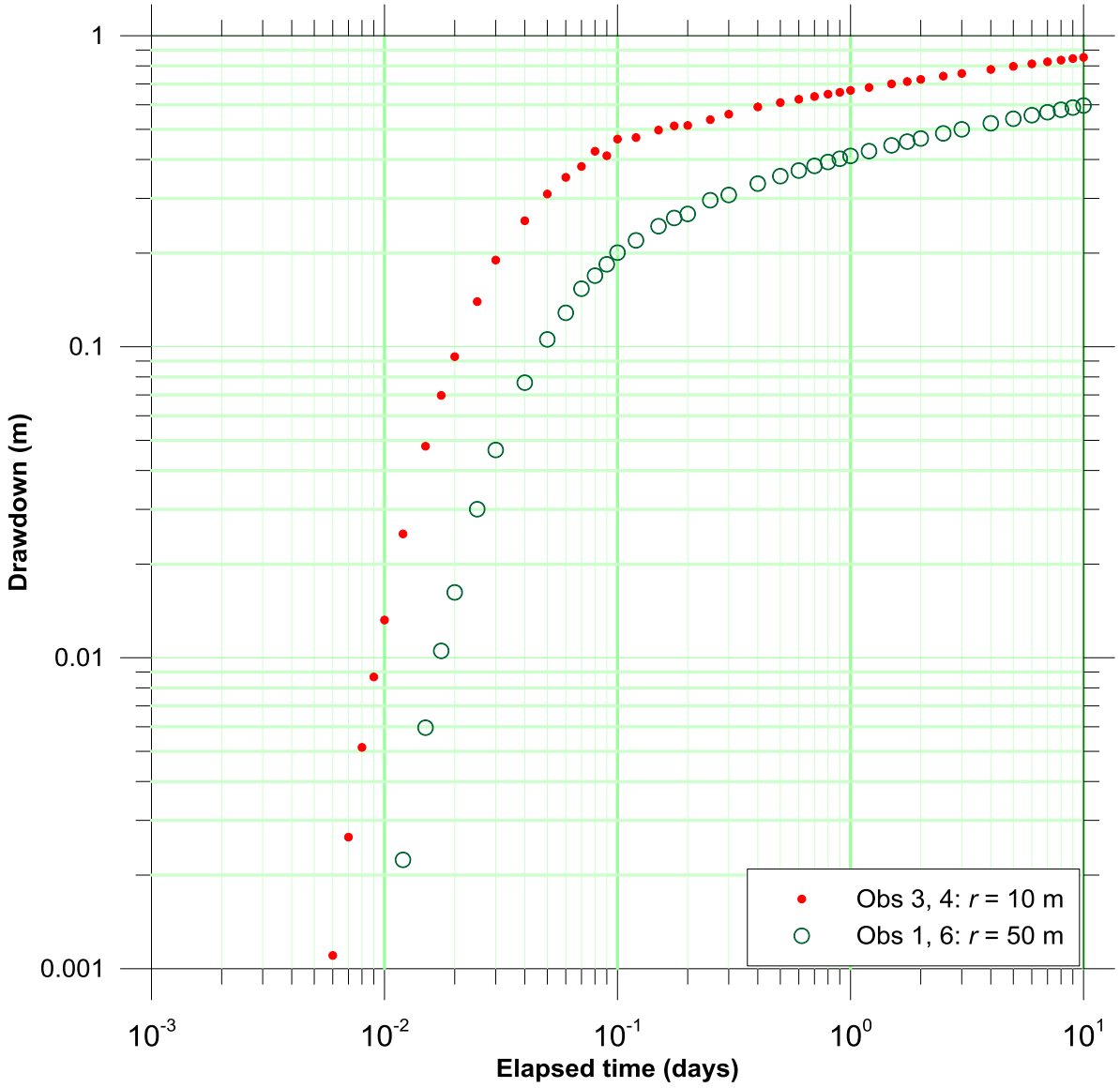

Figure 20. Simulated drawdowns at observation wells #1 and #3 (*r* = 50 m and 10 m)

The match of the Theis solution to the simulated drawdowns at the two observation wells located 10 m from the pumping well is shown in Figure 21. The dashed line represents the "best fit" obtained with a nonlinear regression routine. The match shown is a "best fit" only in a statistical sense, as the solution does not match any portion of the response particularly well. The estimated transmissivity is 64 m^2/d, which is not representative of the transmissivities of either the formation or the pod.

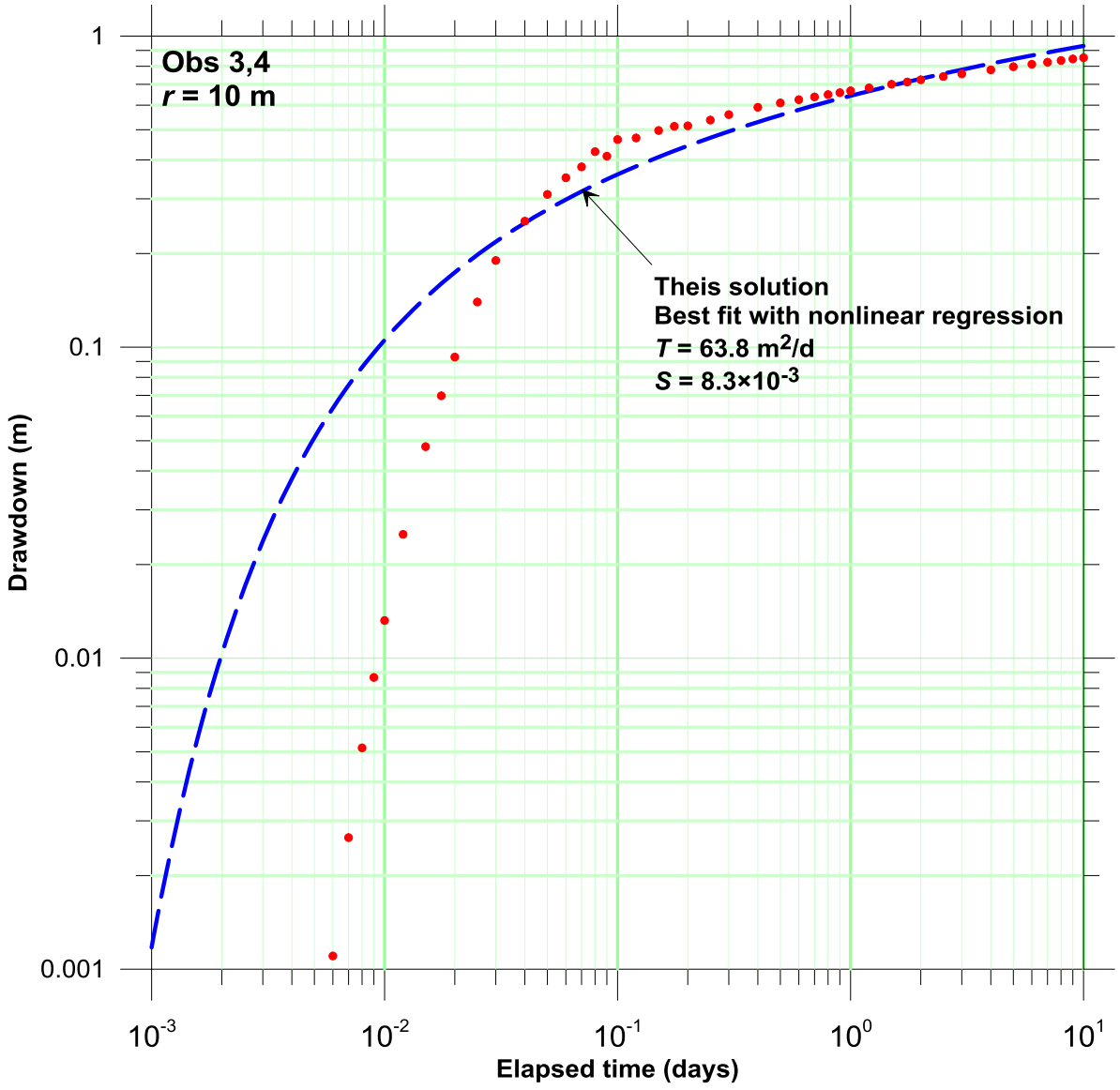

Figure 21. Match of the Theis solution to the drawdowns at observation wells at *r* = 10 m

In Figure 22, the Theis solution evaluated with the parameters corresponding to the formation is superimposed on the simulated drawdowns at r = 10 m. The Theis solution for a uniform aquifer matches closely the drawdowns beyond 0.1 days; however, it is unlikely that an analyst would be willing to accept the apparent poor match to the earlier drawdowns.

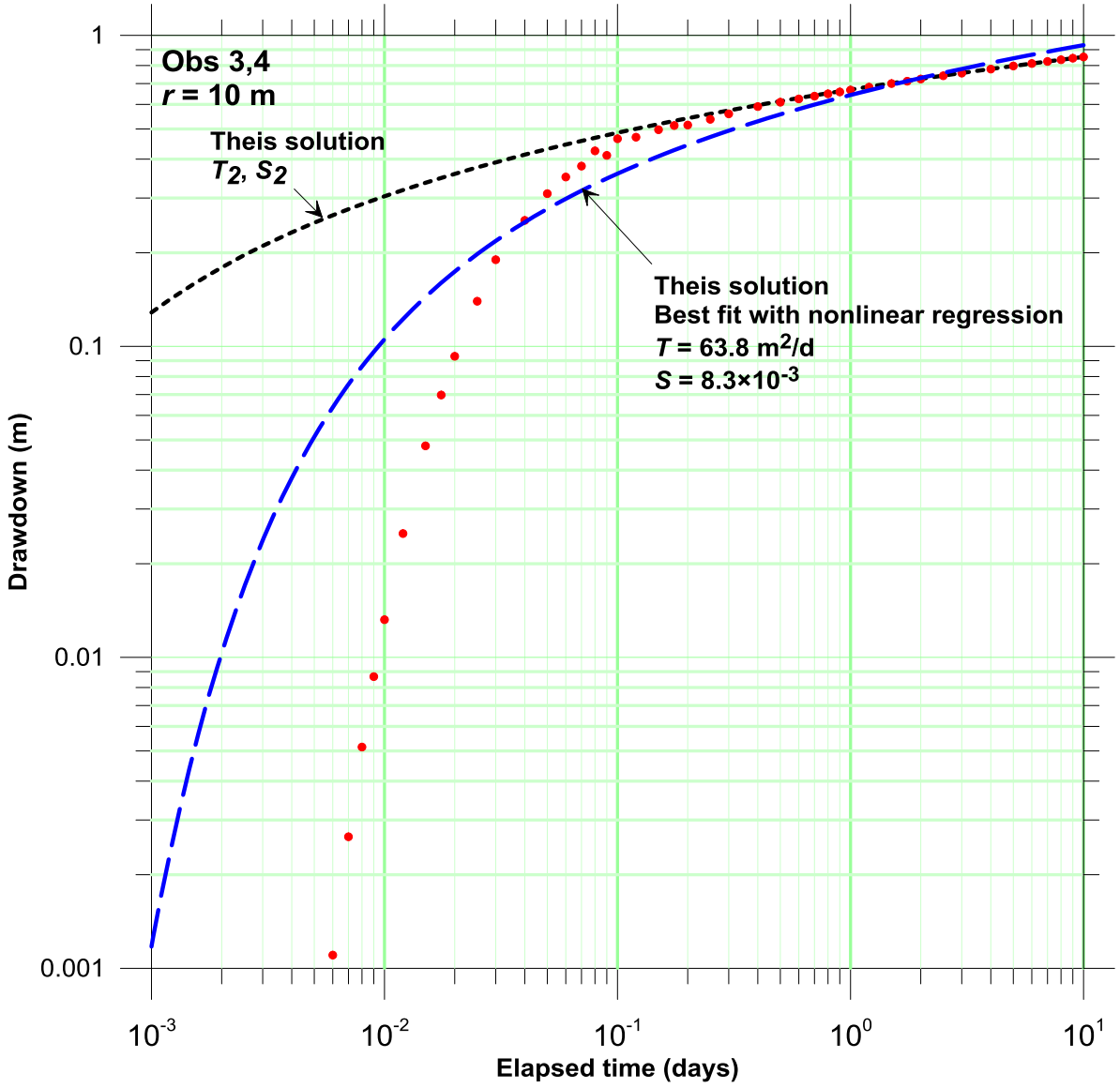

Figure 22. Theis solution with formation parameters, observation wells at r = 10 m

The match of the Theis solution to the simulated drawdowns at the two observation wells located 50 m from the pumping well is shown in Figure 23. The dashed line represents the "best fit" obtained with a nonlinear regression routine. A relatively good match to the simulated drawdowns in achieved after about 0.1 days, with an estimated transmissivity that is about 80% of the value specified for the formation.

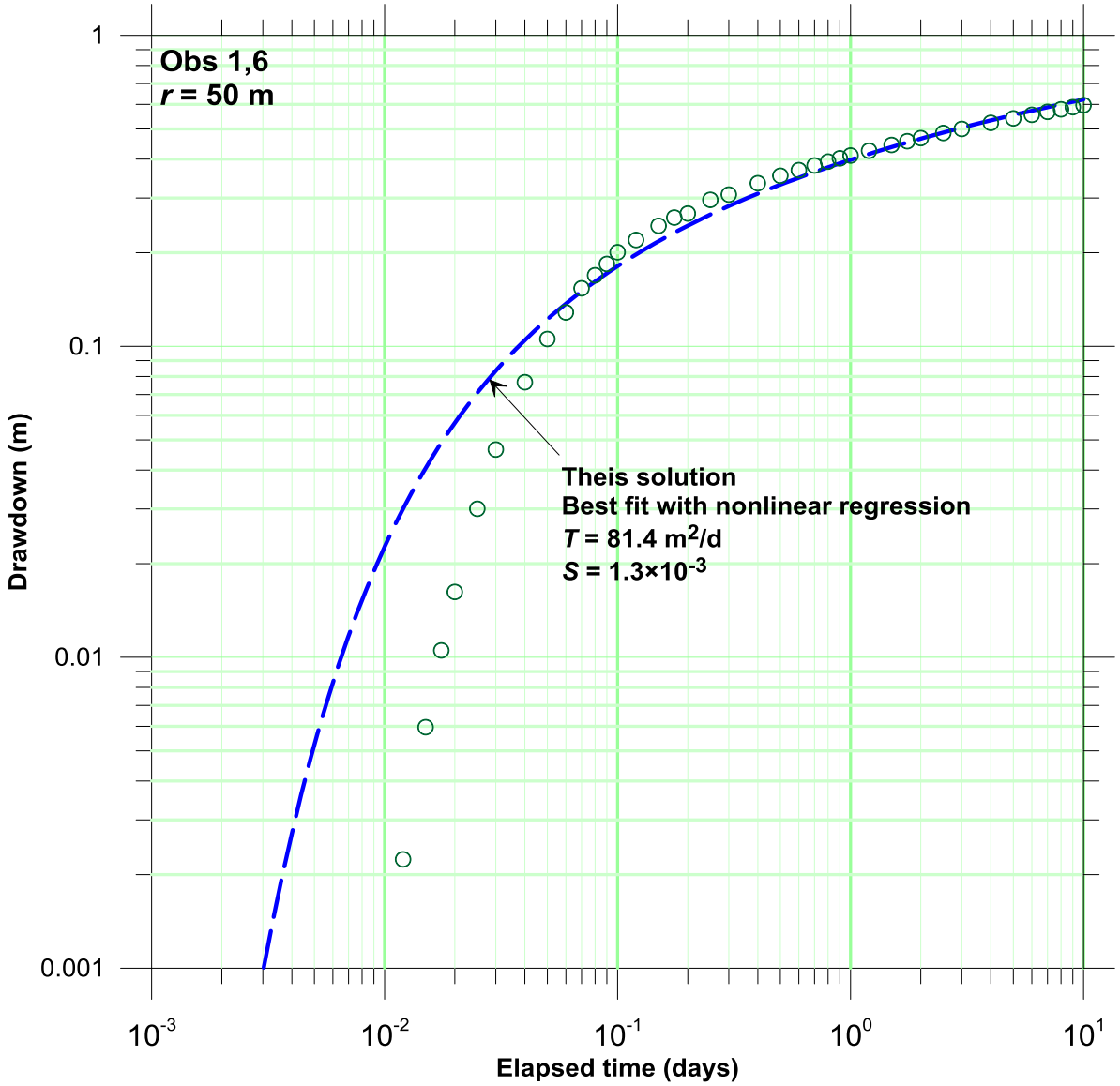

Figure 23. Match of the Theis solution to the drawdowns at observation wells at *r* = 50 m

In Figure 24, the Theis solution evaluated with the parameters corresponding to the formation is superimposed on the simulated drawdowns at r = 50 m. The Theis solution for a uniform aquifer matches closely the last portion of the simulated drawdowns. Again it is unlikely that an analyst would be willing to accept the apparent poor match to much of the drawdowns.

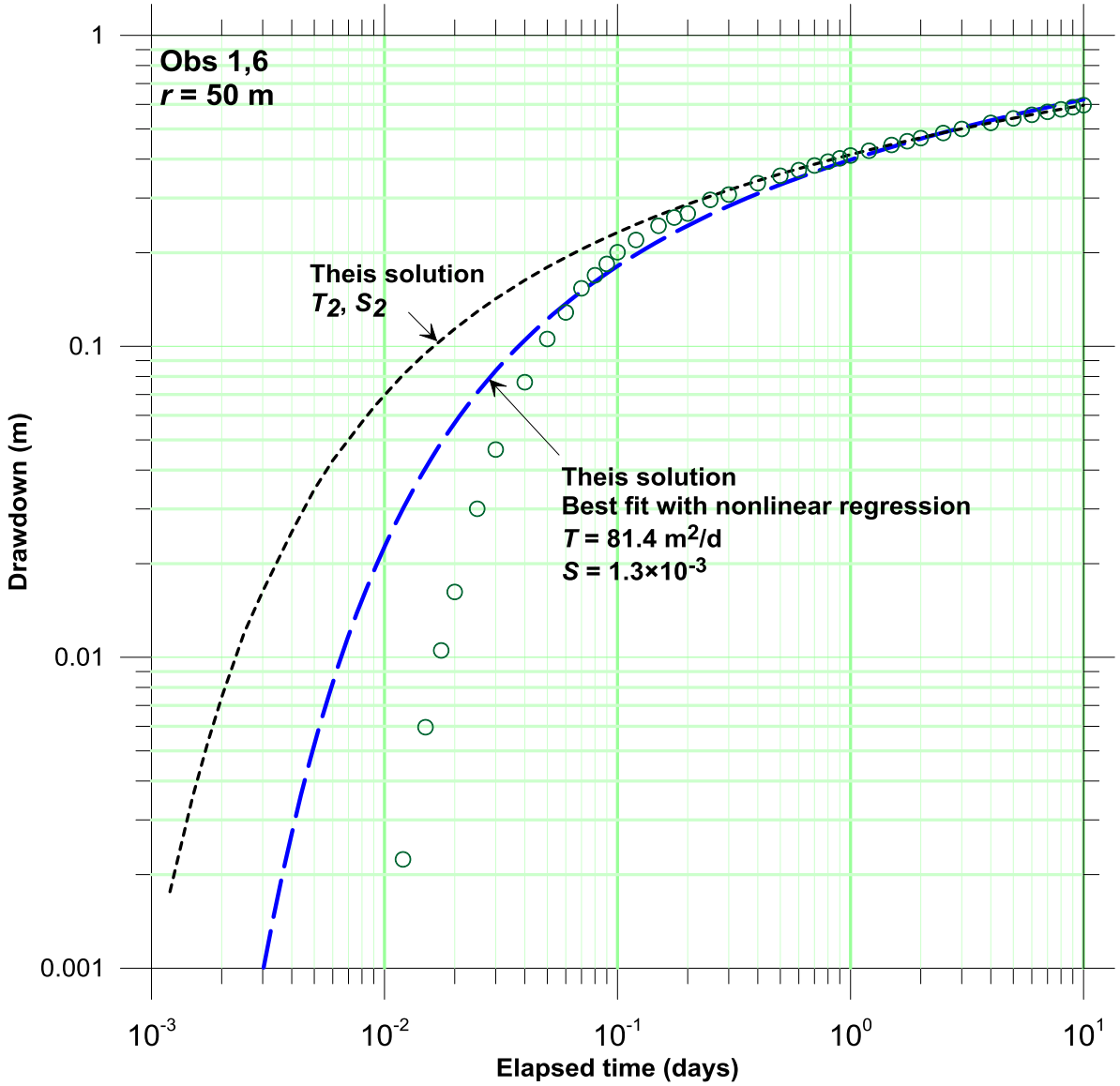

Figure 24. Theis solution with formation parameters, observation wells at r = 50 m

The simulated drawdowns for the observation wells are assembled in a single composite plot in Figure 25. Here the composite semilog plot shows its strengths. The convergence of the simulated drawdowns on a common later-time straight line is evident and there is no ambiguity in identifying the portion of the plot to match to obtain a consistent estimate of the transmissivity.

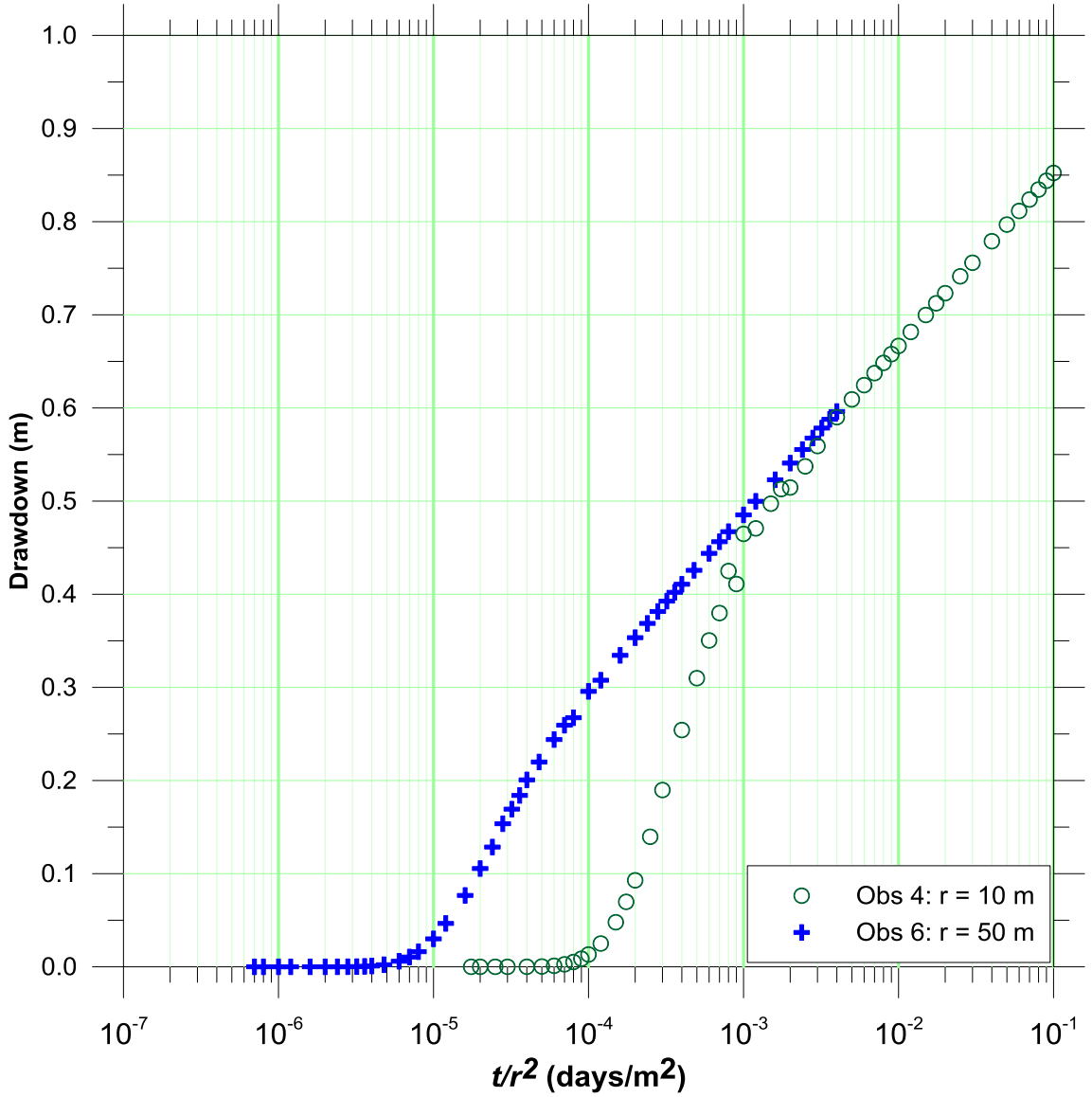

Figure 25. Semilog composite plot for Case #1 pod simulation

The Theis solution for a uniform aquifer evaluated with the parameters for the formation, T_2 and S_2, is superimposed on the simulation results in Figure 26. As shown in the figure, a Cooper-Jacob analysis over the common straight line portion of the two simulated responses would yield an estimate of the transmissivity identical to that specified for the formation.

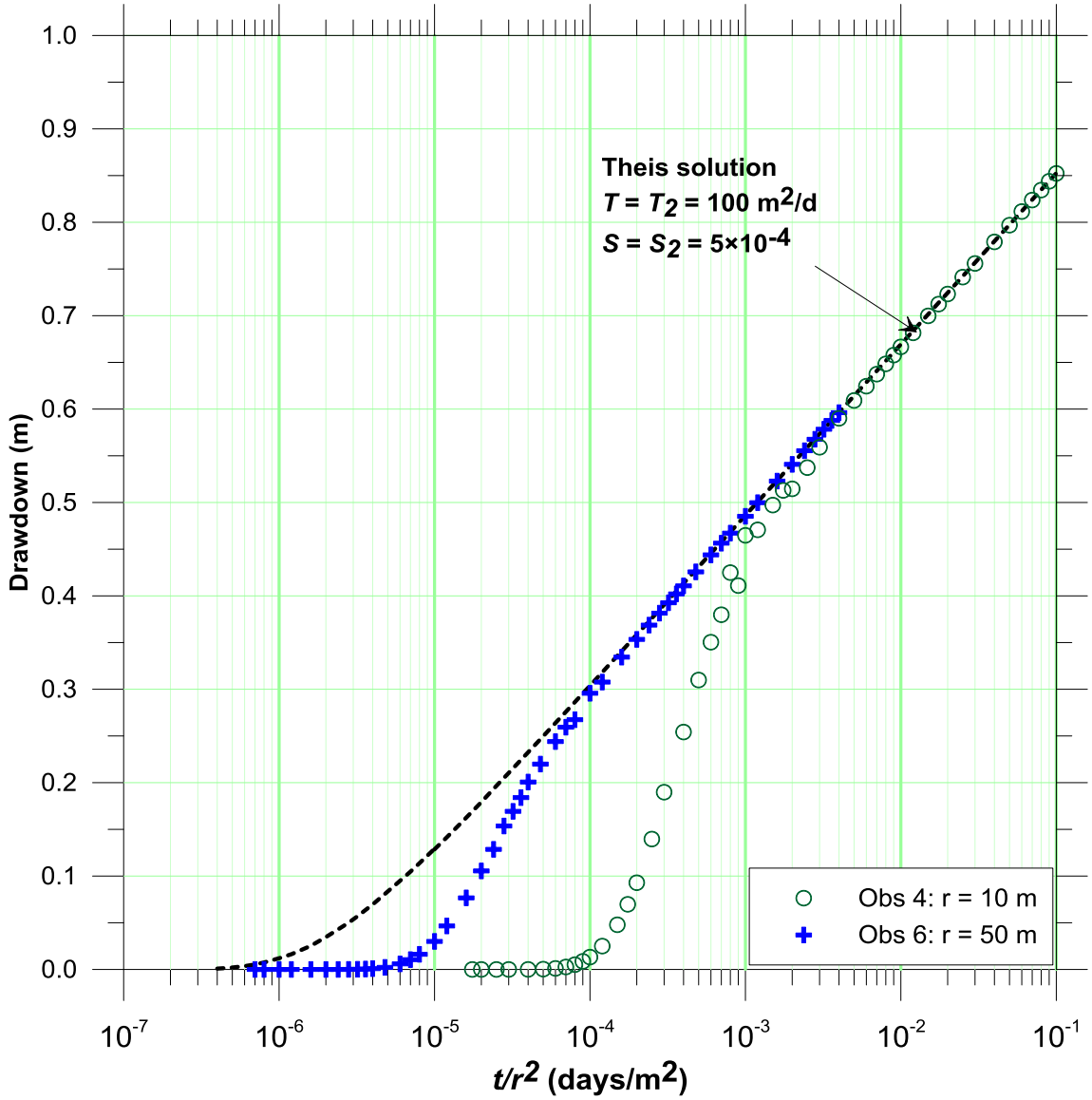

Figure 26. Semilog composite plot for Case #1 with Theis solution for a uniform aquifer

Case #2: Observation well located in a pod

The conceptual model for the second case is shown schematically in Figure 27. The transmissivity of the formation is 100 m^2/day (T_2). Observation wells #3 and #4 are located at the same distance from the pumping well (10 m), as are observation wells #1 and #6 (50 m). Observation well #1 is located at the center of a circular pod of 10 m radius with a lower transmissivity, T_1 = 0.1 m^2/day. The storage coefficient is uniform, $S_1 = S_2 = 5\times10^{-4}$. The well is pumped at a constant rate of 100 m^3/day.

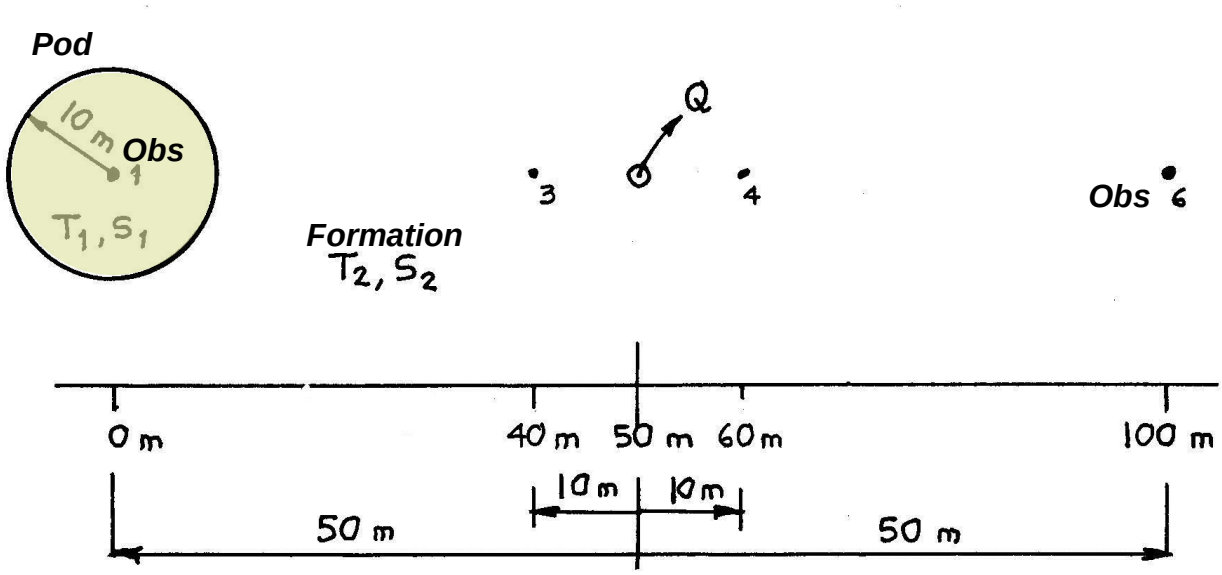

Figure 27. Conceptual model for Case #2 pod simulation

The simulated drawdowns for observation wells #3 and #4 are plotted in Figure 21. The drawdowns are essentially identical, which suggests that the observation wells are not affected by the presence of the pod.

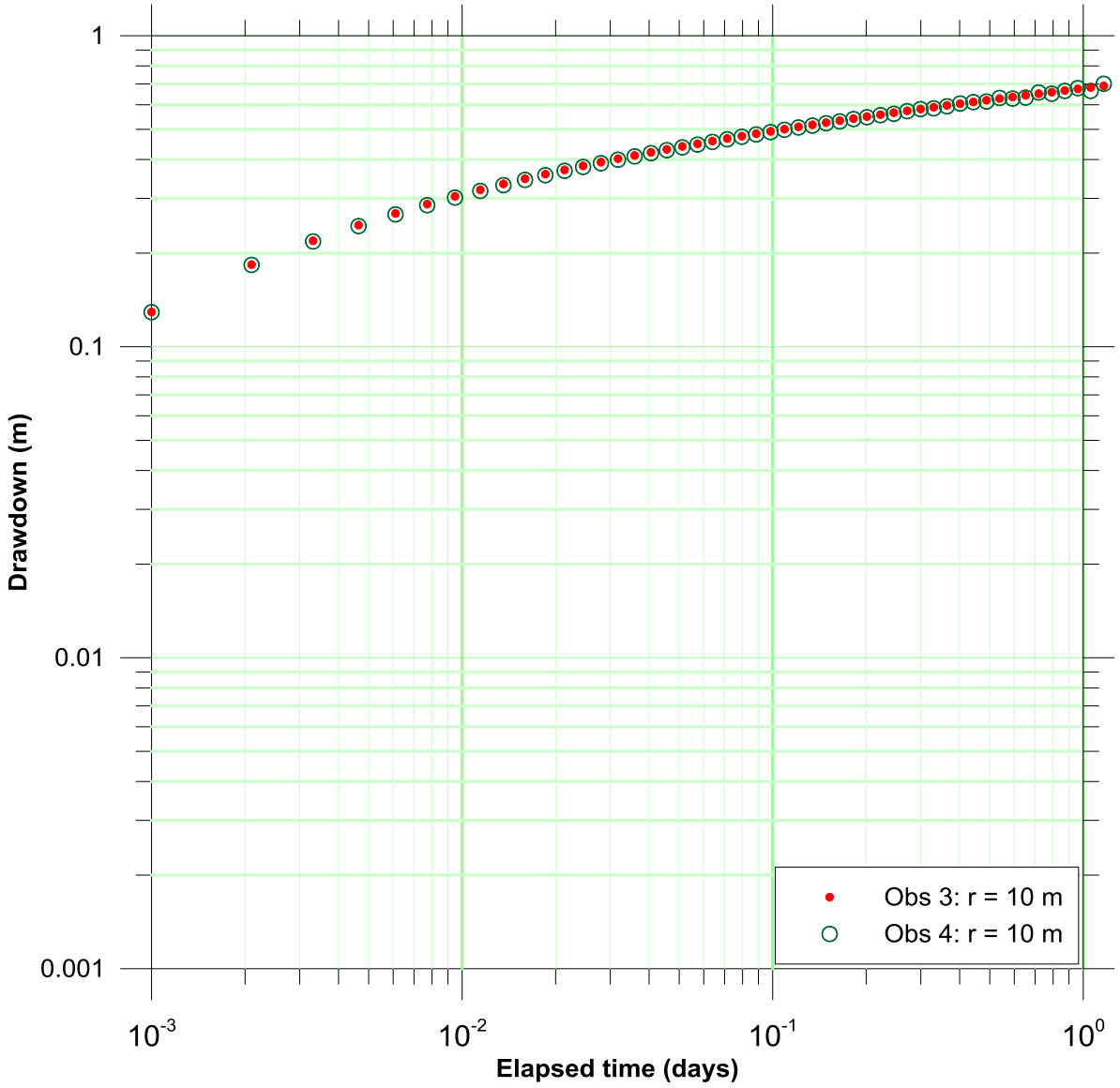

Figure 28. Simulated drawdowns at observation wells #3 and #4 (*r* = 10 m)

In Figure 29 the Theis solution evaluated at r = 10 m with the formation properties, T_2 and S_2, is superimposed on the simulated drawdowns at observation wells #3 and #4. The Theis solution matches closely the simulated drawdowns closely.

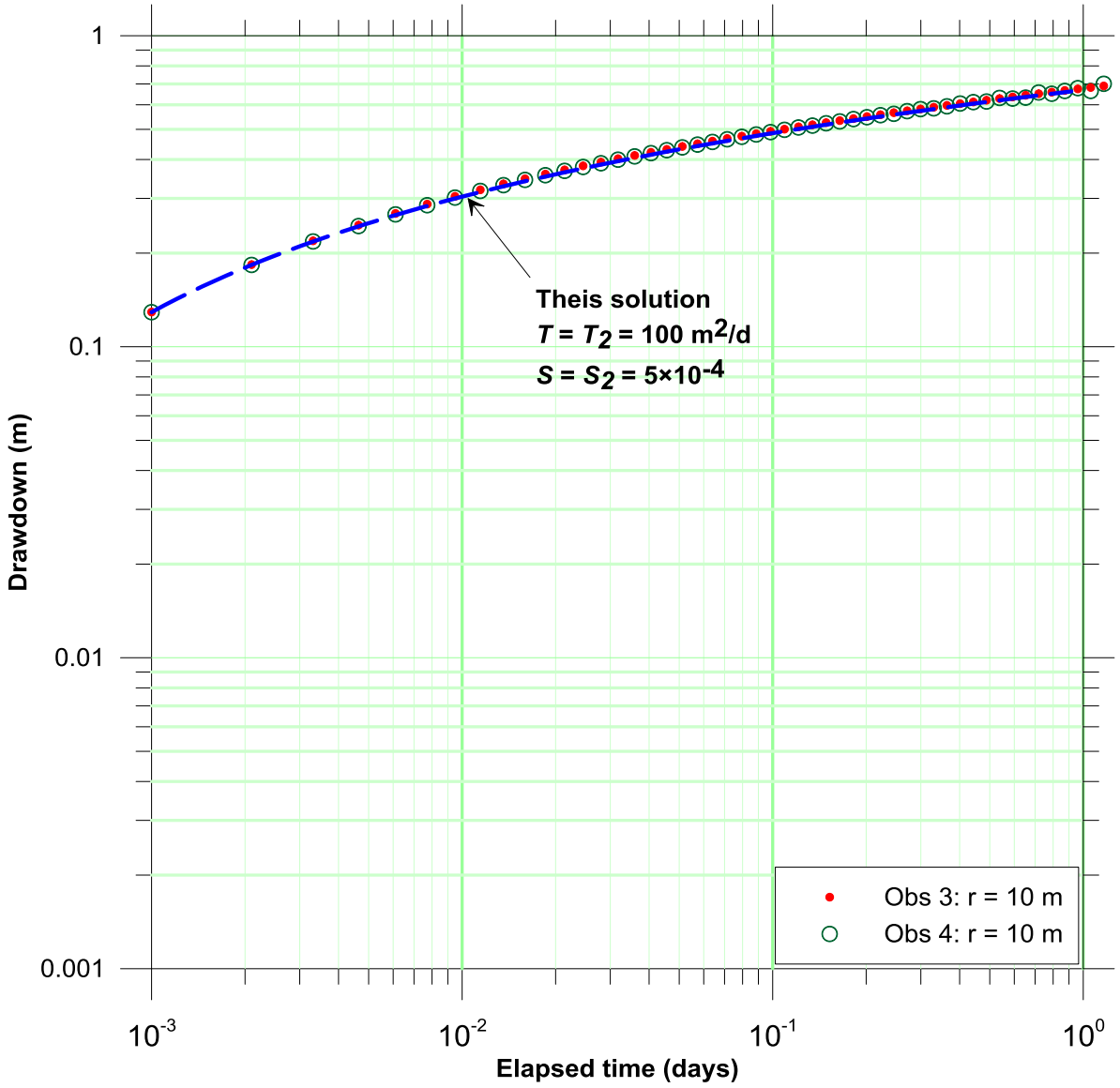

Figure 29. Match of the Theis solution to the drawdowns at observation wells at r = 10 m

The simulated drawdowns at wells located 50 m from the pumping well are plotted in Figure 30. The simulated responses for the two wells are quite different.

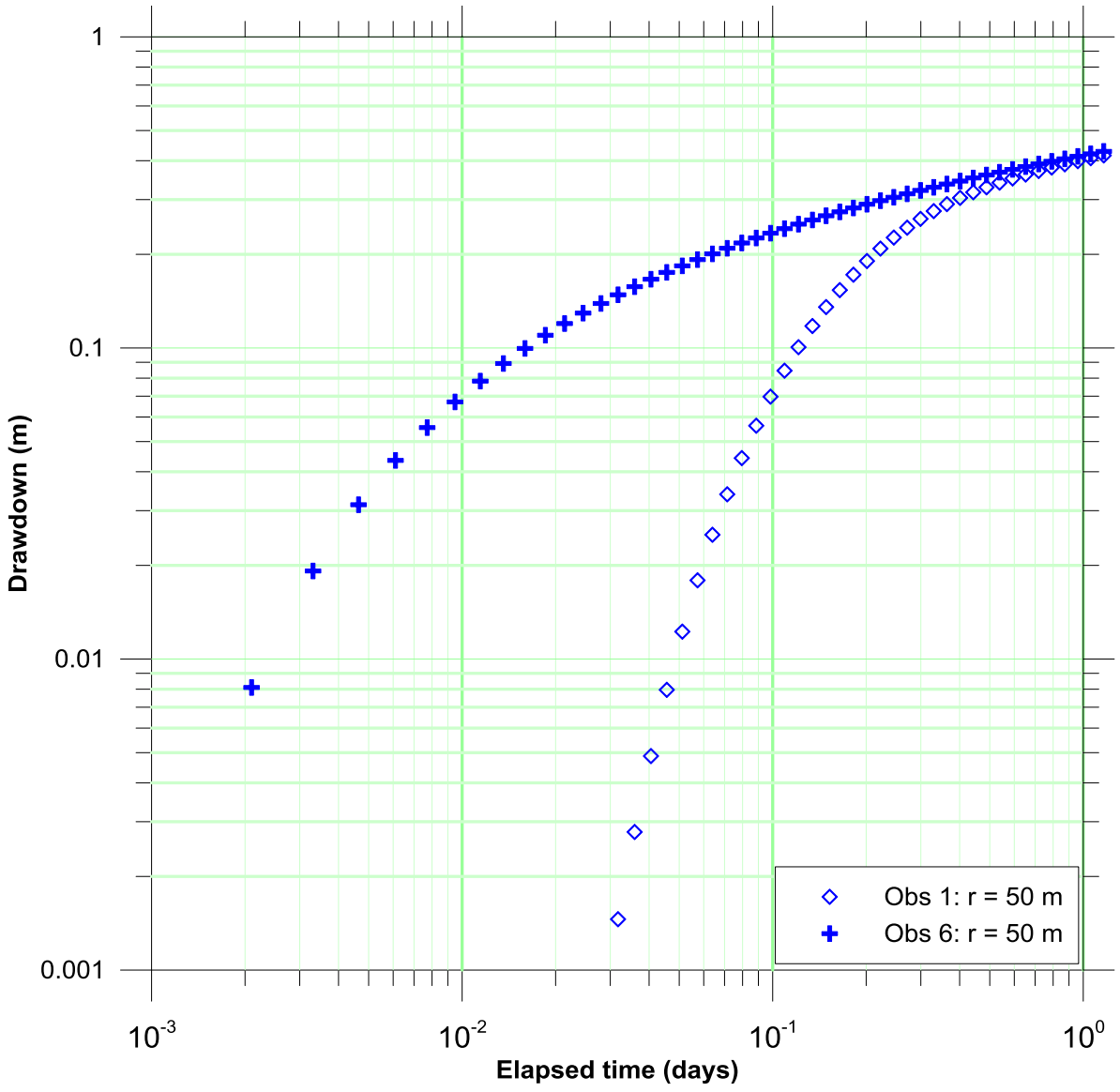

Figure 30. Simulated drawdowns at observation wells #1 and #6 (*r* = 50 m)

Theis analyses for the individual wells at a distance of 50 m are shown in Figures 31 and 32.

The match to the drawdowns at observation #6 with the Theis solution yields the parameter values specified for the formation.

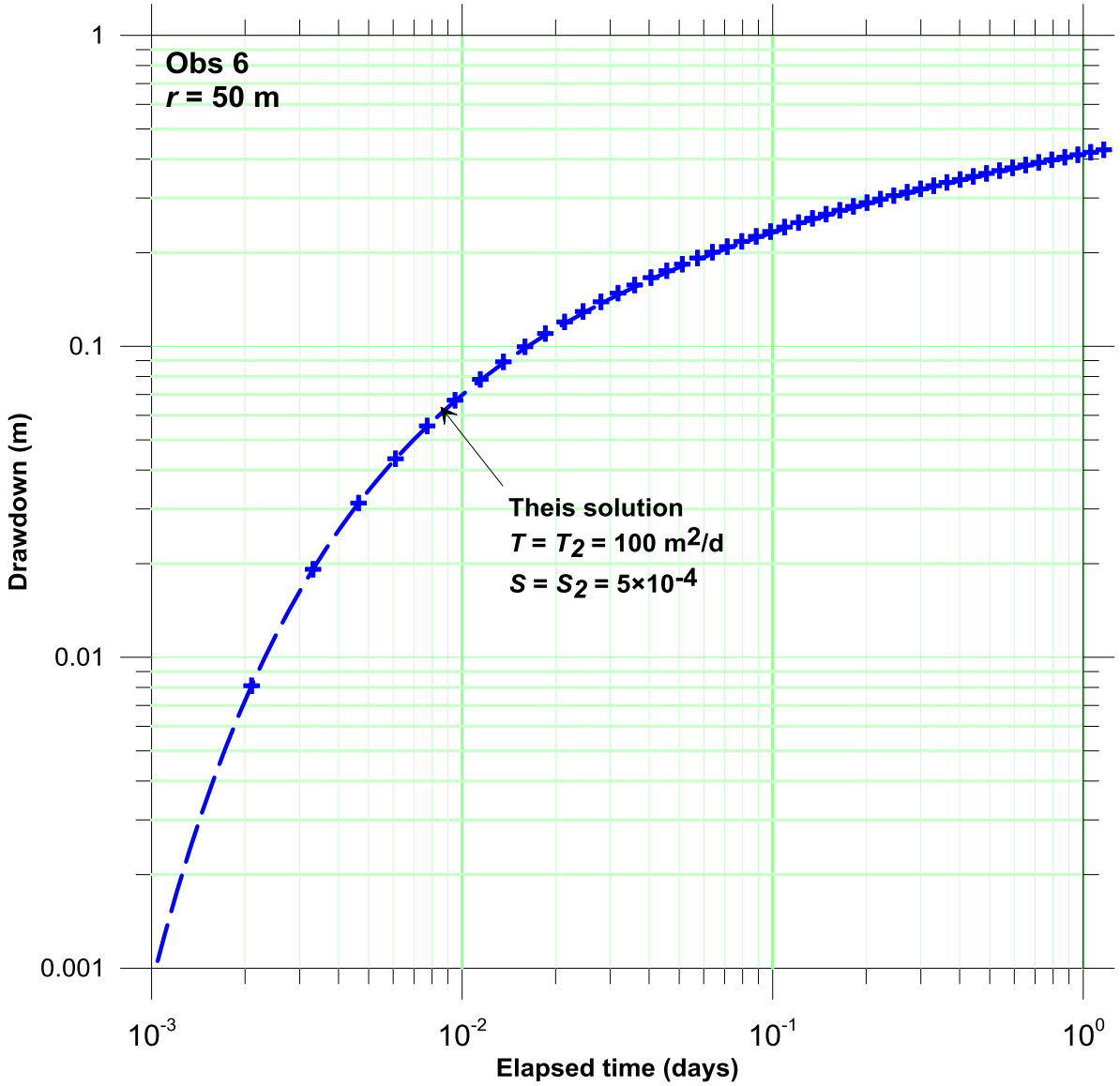

Figure 31. Theis analyses for observation well #6 (*r* = 50 m)

In contrast to the results of the analysis for well #6, it is not possible to achieve a good match to the calculated drawdowns at observation well #1 with any combination of values of *T* and *S*. The best fit analysis obtained with nonlinear regression shown in Figure 32 yields a transmissivity of 42 m^2/d. Since the correct parameter values are already known, we can conclude that the transmissivity estimated for well #1 is not representative of either the formation or the pod in which it is located. Without the benefit of the correct parameter values, it would only be possible to note that something is amiss, as the fit is poor and the estimated transmissivity is significantly different than the value estimated for wells #3, 4, and 6.

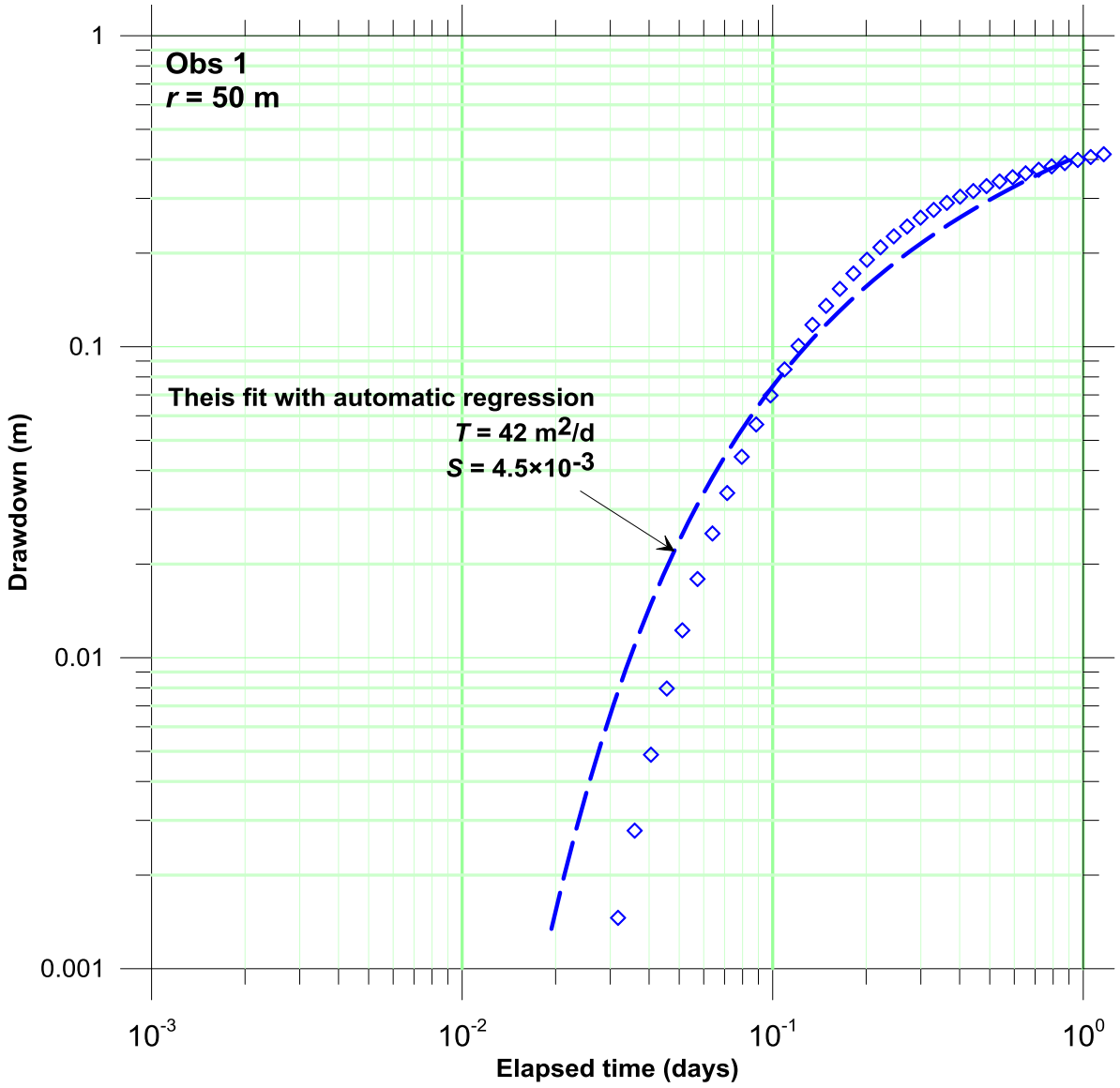

Figure 32. Theis analyses for observation well #1 (*r* = 50 m)

The simulated drawdowns for the four observation wells are assembled in a semilog composite plot in Figure 33. In the figure, the drawdowns for three of the wells approximate the same line, while the early-time drawdowns for observation well #1 appear to be anomalous. The composite plot reveals that matching the early-time observations from well #1 is not appropriate.

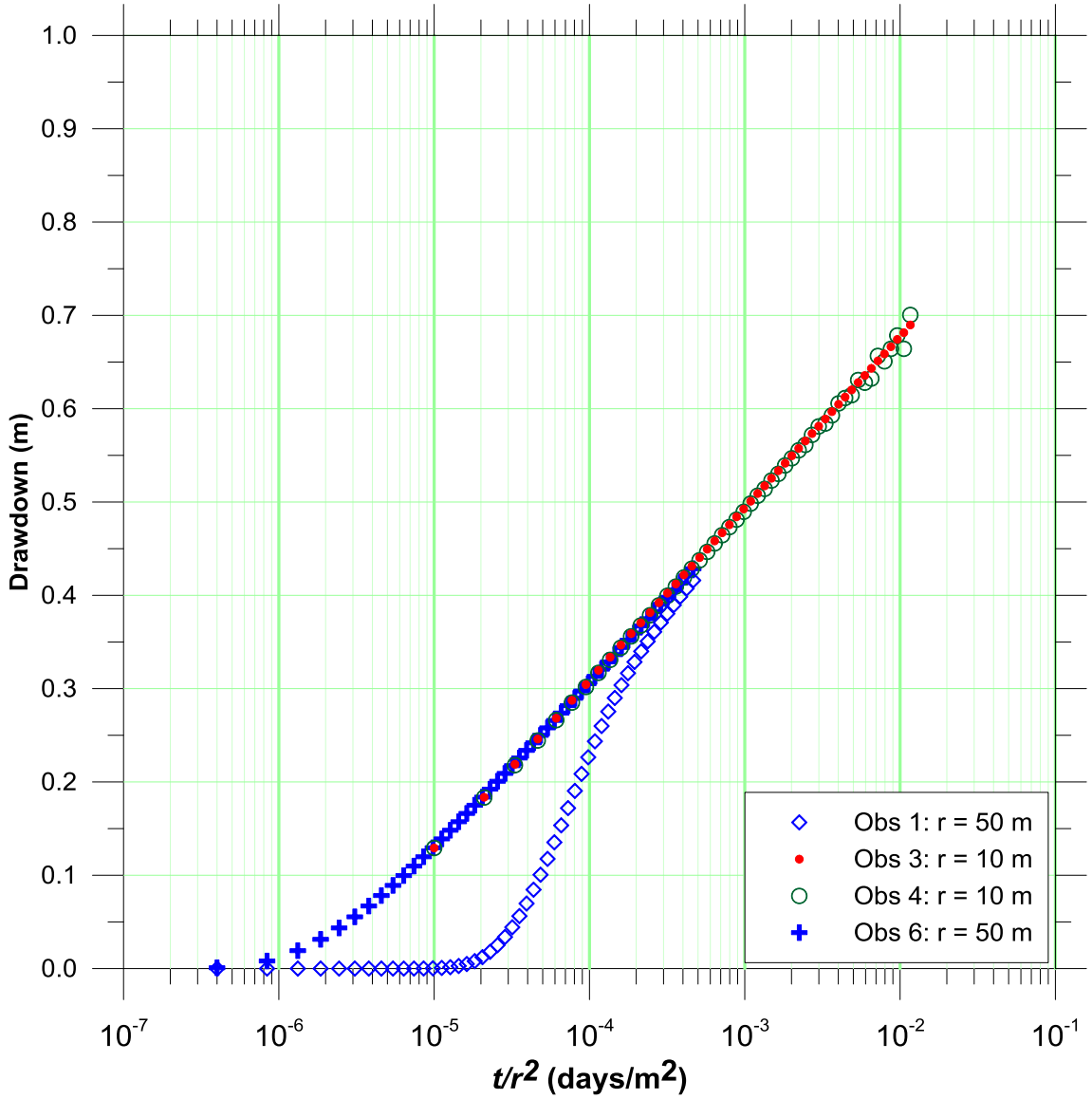

Figure 33. Semilog composite plot for Case #2 pod simulation

As shown in Figure 34, the simulated drawdowns converge on the results predicted for a homogeneous aquifer with the properties of the formation. A Cooper-Jacob analysis conducted on the late-time data would yield an estimate of the transmissivity that is consisent with the value specified for the formation.

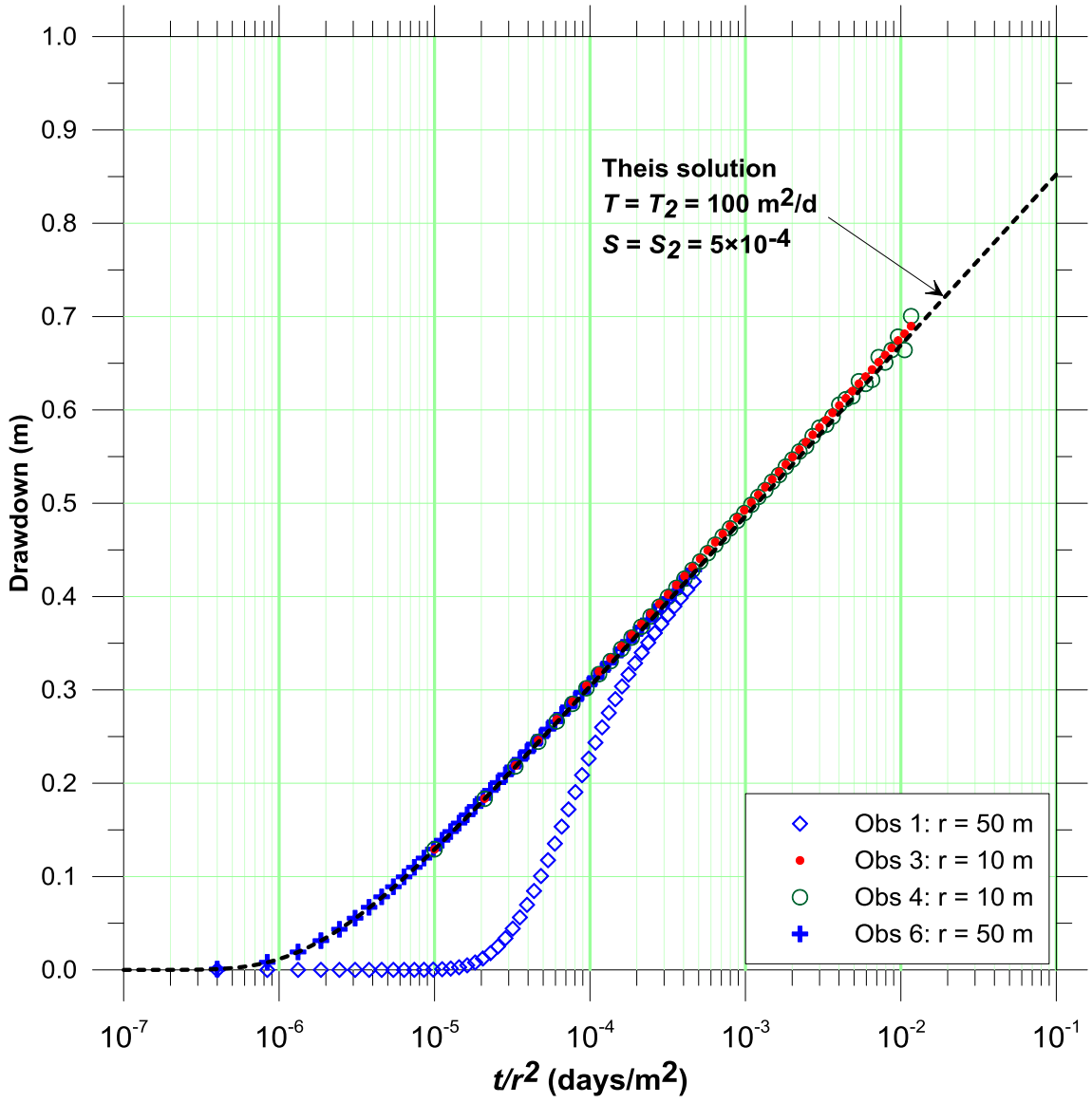

Figure 34. Semilog composite plot for Case #2 pod simulation

Tentative conclusion:

In aquifers that contain distinct zones it may be possible to take advantage of the strengths of the Cooper-Jacob composite analysis to identify the portion of the response that is representative of bulk-average radial flow, and to estimate a representative transmissivity from that portion of the data.

The composite plot serves two purposes: it helps to identify the representative transmissivity of the formation, and it serves to highlight that the response at well #1 is anomalous.

5. Case study

Thus far, the utility of the composite semilog plot for the interpretation of pumping tests in heterogeneous aquifers has been illustrated with simulated results from numerical and analytical solutions. A case study from a pumping test conducted in dolostone rocks of southern Ontario is now considered. The objective of the analyses is to synthesize all of the data with a conceptual model that is internally consistent.

Well NDPW1-08 was installed and tested as part of a program to investigate additional municipal groundwater supplies for Cambridge, Ontario. NDPW1-08 was pumped for 6 days at an average rate of 50 L/s (4,320 m^3/d). The drawdowns were recorded at the pumping well and at 9 observation wells. The distances between the pumping well and the observation wells ranged from 3.54 m to 3,720 m and are tabulated below.

Well	Distance from NDPW1-08, *r* (m)
NDPW1-08	0.15
NDTW2A-08	3.54
NDTW1A-08	156.79
NDOW1A-08	664.43
NDOW2A-08	1042.13
CMOW1A-06	3707.77
CMOW2A-06	2631.96
CMPW2-06	3274.02
PBOW1A-06	3542.39
SMTW1A-05	3720.39

The time-drawdown records are shown in Figure 27. The results of a step test conducted on the pumping well have been used to estimate the nonlinear well loss coefficient, *C*, and to remove the nonlinear well losses from the pumping well drawdowns.

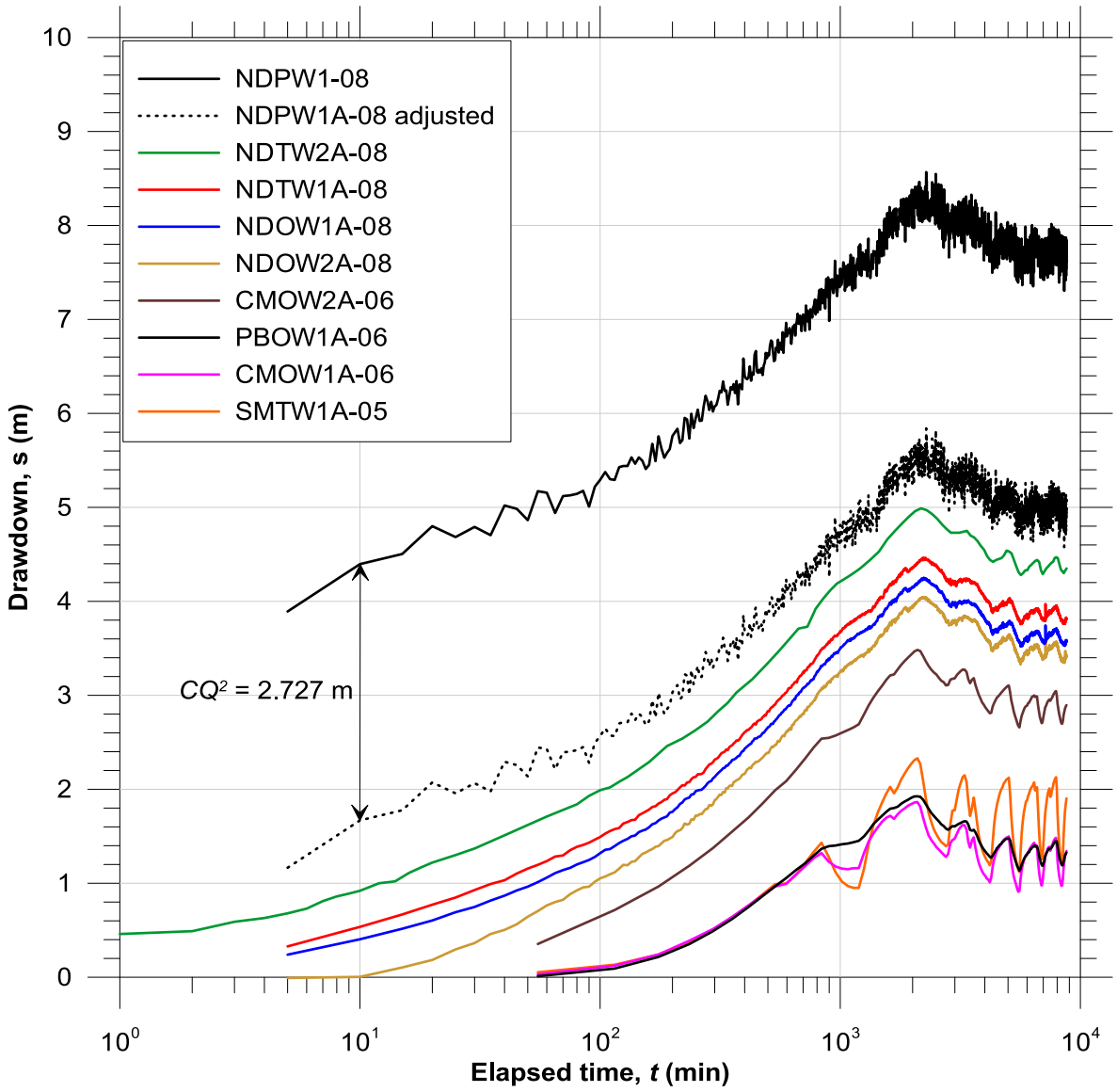

Figure 27. Drawdown versus time for the pumping and observation wells

The corresponding composite plot for the test is shown in Figure 28.

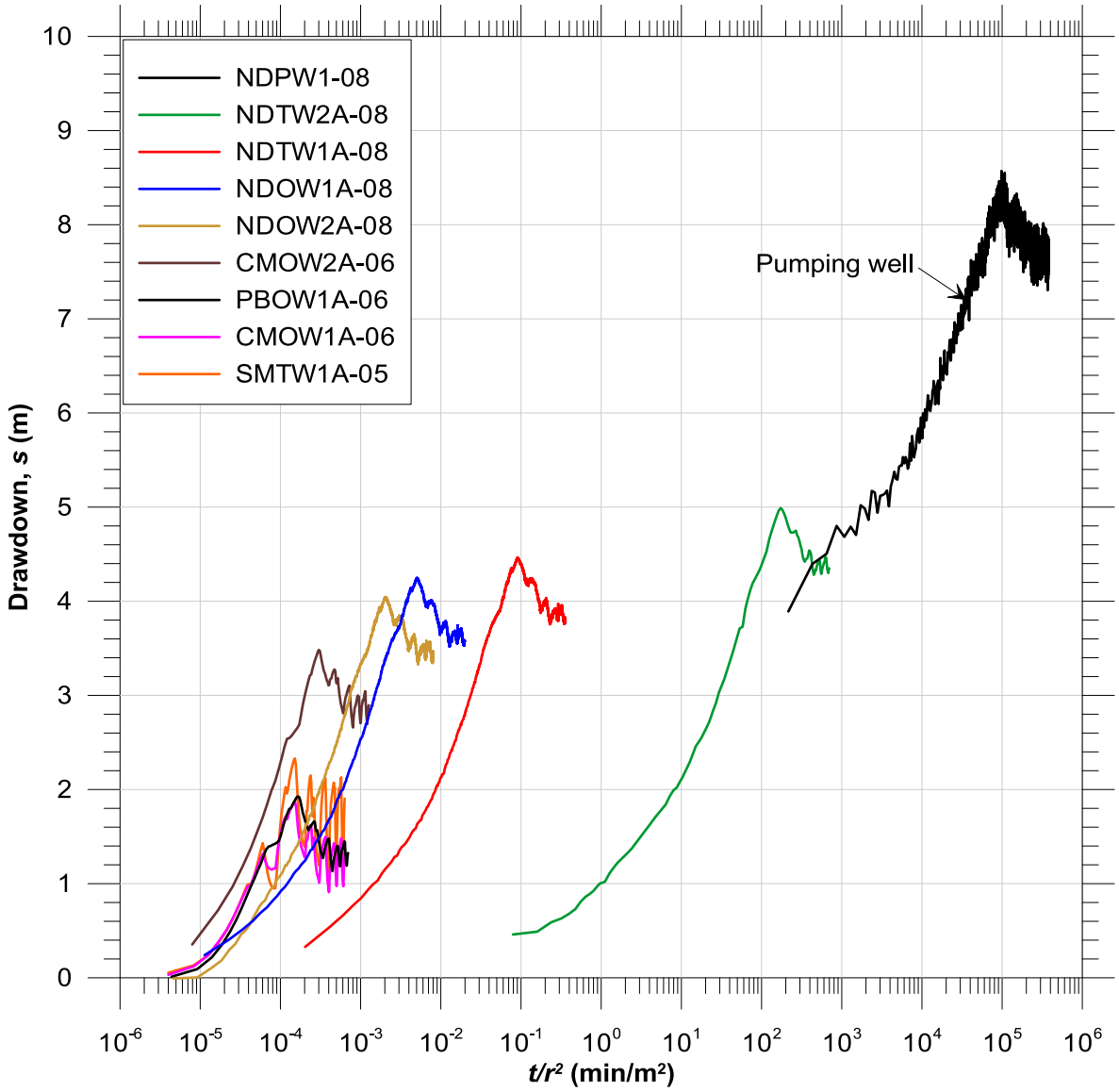

Figure 28. Composite plot for the constant-rate pumping test

The data presented in Figure 28 suggest that it is straightforward to obtain a consistent estimate of the bulk-average transmissivity, as all of the observation wells have similar semilog slopes. This is illustrated in Figure 29, in which straight lines with identical slopes are superimposed on the individual records. In this case, the slope is 2.6 m per log cycle t/r^2, which yields a transmissivity of 305 m^2/d.

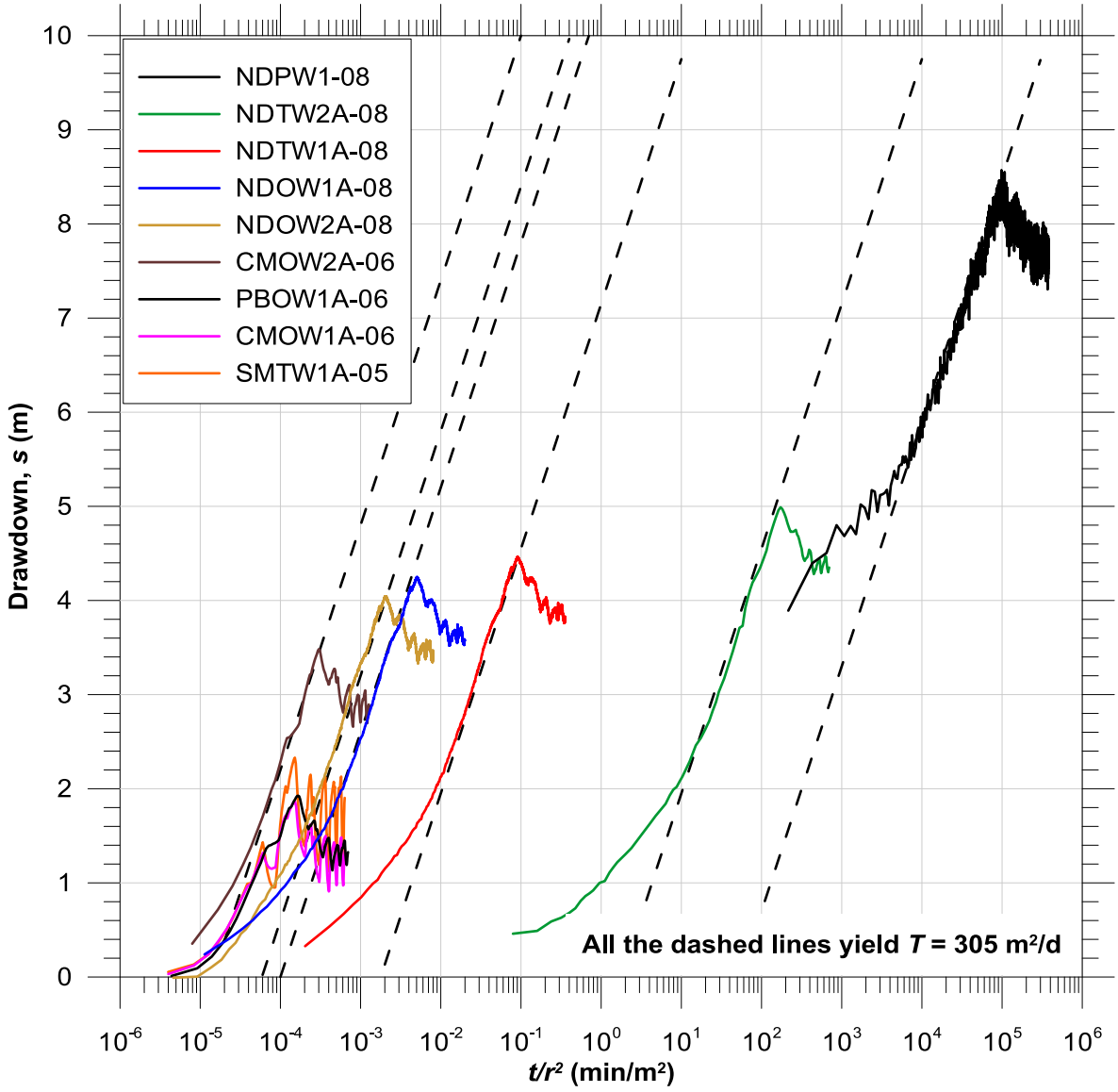

Figure 29. Composite plot with Cooper-Jacob straight-line analysis

If the only objective of the interpretation was to obtain a consistent estimate of the bulk-average transmissivity, the analysis could stop at Figure 29. However, to develop a complete conceptual model of the study area it is also important to understand why the individual wells respond as they do. In this respect, the data assembled on the composite plot are puzzling. For an ideal confined aquifer, the drawdowns for all of the wells should fall on a single straight line. There are almost as many straight lines in Figure 29 as there are observation wells. The variation of the storage coefficients suggests that the structure of the subsurface is significantly more complex than conceived with the Theis model.

To gain more insight into the data set, the individual time-drawdown records are re-examined. Two aspects of the drawdown data are noteworthy. First, the drawdowns are relatively smooth up to about 2000 minutes, beyond which they decline and follow an oscillating pattern. The pumping rate was held constant during the test, so the irregularities are not due to pumping from NDPW1-08. They are likely due to the influence of nearby municipal production wells. Second, the responses of all of the wells appear to track each other closely, both during the "smooth" period and the later period of irregular response.

The wells appear to fall into two general groups:

- Group #1:
  The pumping well and observation wells NDTW2A-08, NDTW1A-08, NDOW1A-08 and NDOW2A-08; and

- Group #2:
  The observation wells PBOW1A-6, CMOW1A-06, and SMTW1A-05. These wells are each more than 3000 m from the pumping well. The irregular responses begin earlier for these wells, which is consistent with their relatively close proximity to another municipal production well.

Well CMOW2A-08 appears to respond as if it were in a transition zone between these two groups.

In a second attempt to gain more insight into the data set, the maximum drawdowns, that is, drawdowns observed after about 2,000 minutes of pumping, are plotted against the distances from the pumping well. The drawdowns appear to approximate two straight lines in the distance-drawdown plot shown in Figure 30. The wells on the first straight line belong to Group #1, and the wells on the second straight line belong to Group #2.

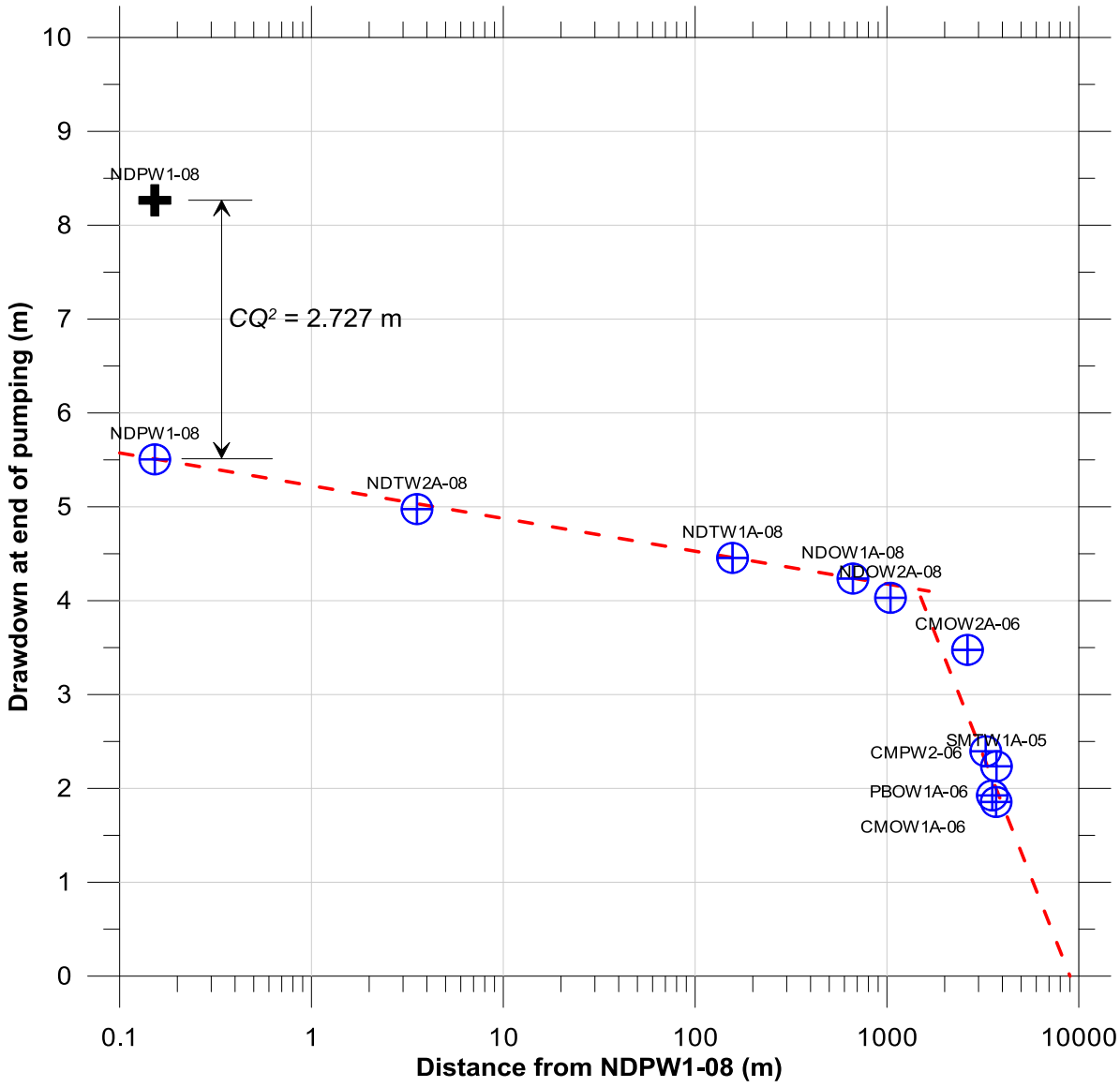

Figure 30. Maximum drawdown versus distance from the pumping well

Following the Cooper-Jacob distance-drawdown analysis, the transmissivity is estimated according to:

$$T = 2.303 \frac{Q}{2\pi} \frac{1}{SLOPE}$$

The slopes of the two dashed lines drawn sin Figure 30 yield two transmissivity estimates:

SLOPE #1: NDPW1-08 (adjusted) to NDOW2A-08

Well	Radial distance (m)	Drawdown at end of test (m)
NDPW1-08 (adjusted)	0.1524	5.51
NDOW2A-08	664.4	4.24

$$SLOPE_1 = \frac{5.51\,\text{m} - 4.24\,\text{m}}{\log\{664.4\,\text{m}\} - \log\{0.1524\,\text{m}\}} = 0.349\ \text{m/logcycle}\ r$$

$$T = 2.303 \frac{4320.6\ \text{m}^3/\text{d}}{2\pi} \frac{1}{0.349\,\text{m}}$$

$$= 4540\ \text{m}^2/\text{d}$$

SLOPE #2: CMOW2A-06 to CMOW1A-06

Well	Radial distance (m)	Drawdown at end of test (m)
Intersection with Line 1	1460.0	4.10
Zero drawdown	9000.0	0.00

$$SLOPE_2 = \frac{4.10\,\text{m} - 0.00\,\text{m}}{\log\{9000\,\text{m}\} - \log\{1460.0\,\text{m}\}} = 5.190\ \text{m/logcycle}\ r$$

$$T = 2.303 \frac{4320.6\ \text{m}^3/\text{d}}{2\pi} \frac{1}{5.190\,\text{m}}$$

$$= 305\ \text{m}^2/\text{d}$$

The transmissivity estimated from the more distant wells is identical to the transmissivity estimated from the composite analysis presented in Figure 29.

To assess whether the inferences from the distance-drawdown analysis might be reliable, the observed drawdowns are simulated with an analytical solution based on a slightly more complex conceptual model. The assumptions of the Theis model are still invoked, with the exception of the assumption of homogeneity. The aquifer is assumed to consist of a zone with one set of properties surrounding the pumping well, surrounded by a zone of uniform properties corresponding to the bulk formation.

- Inner zone: $r < R$, $T = T_1$, $S = S_1$
- Outer zone (formation): $r > R$, $T = T_2$, $S = S_2$

The analytical solution for this problem has been derived independently by Loucks and Guerrero (1961), Barker and Herbert (1982), and Butler (1988).

For simplicity it is assumed that the storage coefficients S_1 and S_2 are both 10^{-5}. Referring to the distance-drawdown plot, Figure 30, it is further assumed that the zone around the pumping well extends for a radial distance of 1460 m. The transmissivity values obtained from Cooper-Jacob distance-drawdown analysis, T_1 = 4540 m^2/d, and T_2 = 305 m^2/d. In Figure 31 the results of the analytical solution are superimposed on the distance-drawdown data. As shown in the figure, an excellent match is obtained to the final drawdowns.

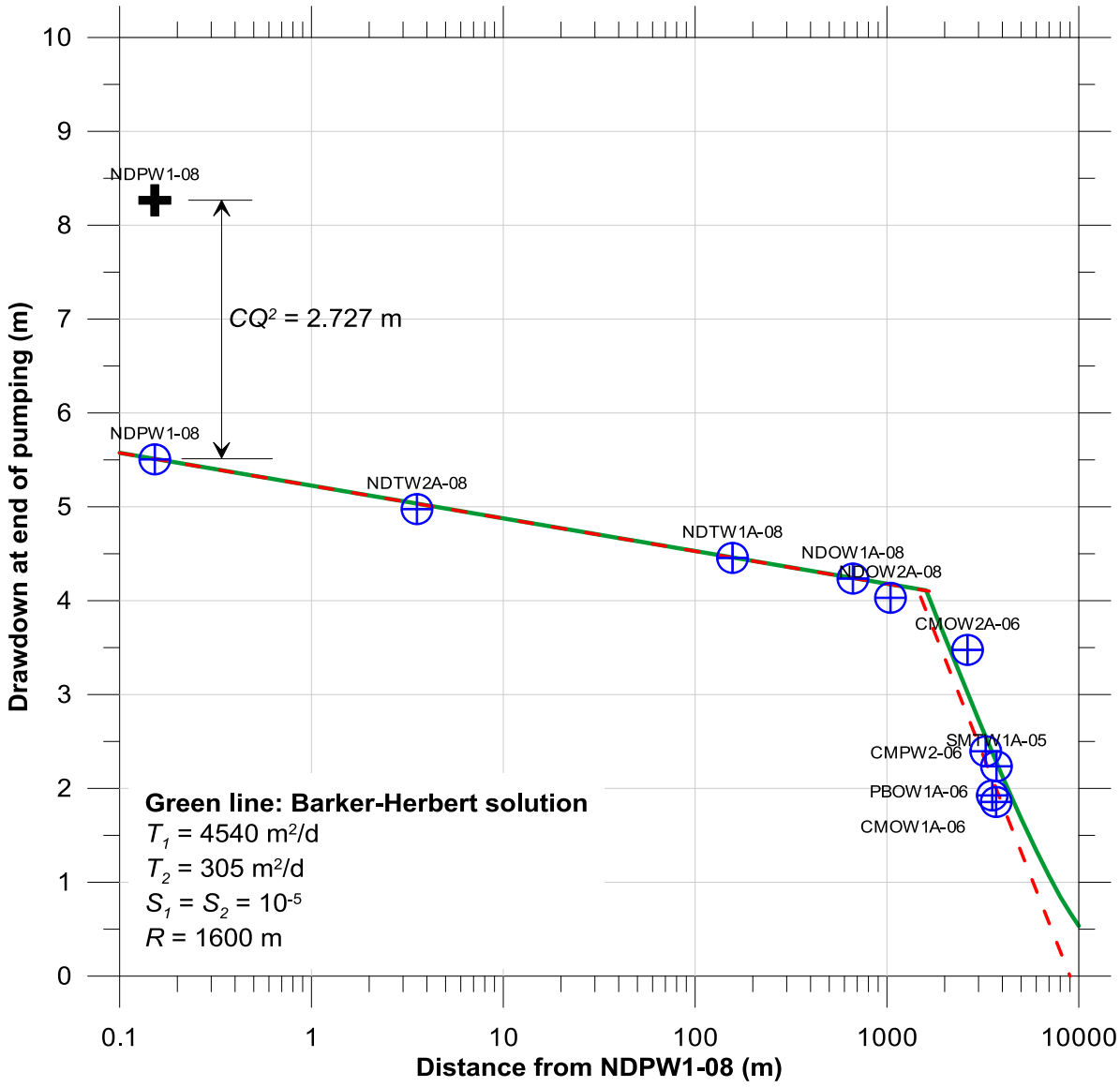

Figure 31. Match to drawdowns with analytical solution of Barker and Herbert (1982)

The match to the final drawdowns is encouraging. But what do the matches to the complete time-drawdown records look like? Using the same parameters as for Figure 31, the complete transient results of the Barker-Herbert model are plotted in Figure 32. For simplicity, the results are shown for only three of the wells: the pumping well (adjusted drawdowns), NDTW1A-08 at 156.8 m, and SMTW1A-05 at 3720 m. Excellent matches to the observations are achieved.

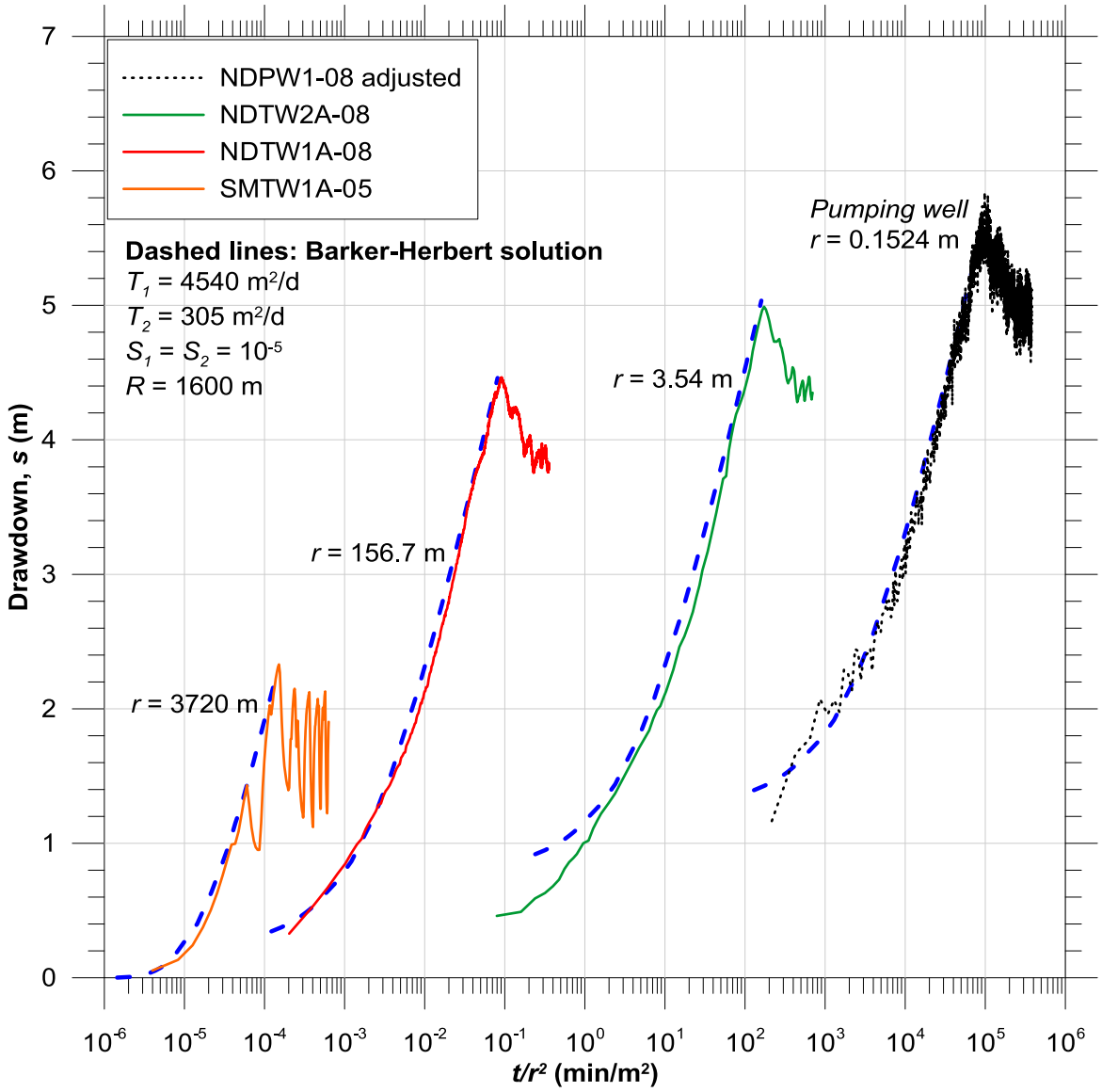

Figure 32. Barker-Herbert solution, composite plot

6. Conclusions

Cooper and Jacob (1946) recommended that when time-drawdown records are available from multiple wells, the drawdown data should be assembled on a composite plot.

The results of numerical experiments of Meier and others (1998) for statistically homogeneous aquifers and simulations developed with the "pod" analytical solutions of Butler and Liu (1993) yield a consistent impression: it may be possible to estimate an effective transmissivity from a pumping test using the Theis model when applied with the semilog composite plotting approach.

The semilog composite plotting approach has two important attributes:

- When applied correctly with a focus on later-time data, a Cooper-Jacob analysis on a semilog composite analysis allows the analyst to look beyond the variability of the responses at individual observation wells. The composite plotting approach directs the analysts towards developing a single estimate of the transmissivity, consistent with the foundations of the analytical solutions typically used to interpret pumping test data; and

- The composite plot assists in identifying those responses that are significantly different, that is, the outliers.

7. References

Barker, J.A., and R. Herbert, 1982: Pumping tests in patchy aquifers, *Ground Water*, vol. 20, No. 2, pp. 150-155.

Butler, J.J., 1988: Pumping tests in nonuniform aquifers – The radially symmetric case, *Journal of Hydrology*, Vol. 101, pp. 15-30.

Butler, J.J., and W. Z. Liu, 1991: Pumping tests in non-uniform aquifers – The linear strip case, *Journal of Hydrology*, Vol. 128, pp. 69-99.

Butler, J.J., and W. Liu, 1993: Pumping tests in nonuniform aquifers: The radially asymmetric case, *Water Resources Research*, Vol. 29, No. 2, pp. 259-269.

Cooper, H.H., Jr., and C.E. Jacob, 1946: A generalized graphical method for evaluating formation constants and summarizing well-field history, *Transactions of the American Geophysical Union*, vol. 27, no. 4, pp. 526-534.

Loucks, T.L., and E.T. Guerrero, 1961: Pressure drop in a composite reservoir, *Society of Petroleum Engineers Journal*, vol. 1, pp. 170-176.

Meier, P.M., J. Carrera, and X. Sanchez-Vila, 1998: An evaluation of Jacob's method for the interpretation of pumping tests in heterogeneous aquifers, *Water Resources Research*, Vol. 34, No. 5, pp. 1011-1025.

Moench, A.F., 2010: Comment on "Analysis of pumping test data for determining unconfined-aquifer parameters: Composite analysis or not?", *Hydrogeology Journal*, vol. 18, pp. 1975-1977.

Sánchez-Vila, X., P.M. Meier, and J. Carrera, 1999: Pumping tests in heterogeneous aquifers: An analytical study of what can be obtained from their interpretation using Jacob's method, *Water Resources Research*, Vol. 35, No. 4, pp. 943-952.

Theis, C.V., 1935: The relation between the lowering of the piezometric surface and the rate and duration of discharge of a well using ground-water storage, *Transactions of the American Geophysical Union*, 16th Annual Meeting, Part 2, pp. 519-524.

Todd, D.K., and L.W. Mays, 2005: **Groundwater Hydrology**, 3rd edition, John Wiley & Sons, Inc., Hoboken, New Jersey.

Weeks, E.P., 1977: Aquifer Tests – The state of the art in hydrology, in *Proceedings of the Invitational Well-Testing Symposium*, Berkeley, California, October 19-21, 1977, pp. 14-26.